Papers

International Journal of Bifurcation and Chaos, Vol. 9, No. 4 (1999) 591–616

CHUA SYSTEMS WITH DISCONTINUITIES

C.-H. LAMARQUE, O. JANIN and J. AWREJCEWICZ
Ecole Nationale des Travaux Publics de l'Etat, LGM – URA CNRS 1652,
1 rue Maurice Audin – F69 518 Vaulx-en-Velin, Cedex, France
Technical University of Lódź, Division of Control and Biomechanics,
1/15 Stefanowskiego – 90-924 Lódź, Poland

Received December 16, 1997; Revised September 17, 1998

We present a special class of mechanical systems that could be written as Chua circuits with discontinuities. We recall the general frame for the study of such models. Results of existence and uniqueness are given. Then numerical results obtained via piecewise analytical expressions are presented. We discuss some bifurcation diagrams, phase portraits. Chaos is characterized by computing Lyapunov exponents. We analyze the global behavior in a special case where discontinuity stabilizes the trivial equilibrium solution.

1. Introduction

Many works have been devoted to the study of the global behavior of smooth nonlinear oscillators (Duffing oscillator [Ueda, 1979], shallow arches [Szemplinska-Stupnicka *et al.*, 1989; Lamarque & Malasoma, 1992; Malasoma *et al.*, 1994], Lorentz's system [Lorentz, 1963; Sparrow, 1982], etc.) or smooth maps (logistic map [Coullet & Tresser, 1984; Feigenbaum, 1978], etc.): Both periodic, quasi periodic or chaotic behavior have been investigated, bifurcations, transitions, universal behavior have been studied. At the same time a number of papers deal with "simpler, integrable" systems which seem to be "paradigms": Unimodal maps [Collet & Eckmann, 1980; Li & Yorke, 1975; Sharkovski, 1964], Lozi's attractor [Lozi, 1978], Chua's double scroll circuit [Madan, 1993], etc. Indeed the latter are concerned with piecewise-linear dynamics exhibiting chaotic behavior via analytically built Poincaré maps [Lozi, 1978; Chua *et al.*, 1986; Komuro *et al.*, 1991], etc.

But few studies deal with the bifurcations and the global behavior of unsmooth systems, i.e. systems with mathematical difficulties such as discontinuities and, or multivalued differential equations. Such models are interesting from the point of view of applications: Impacts, friction and constitutive laws provide unsmooth models of that type [Paoli, 1993; Paoli *et al.*, 1992; Monteiro Marques, 1994; Deimling, 1992; Popp & Stelter, 1990; Pfeiffer & Prestl, 1994; Whiston, 1987; Shaw, 1986; Shaw & Shaw, 1989; Dowell & Schwartz, 1983; Ferri & Bindemann, 1995; Moreau, 1988; Awrejcewicz & Delfs, 1990a; Awrejcewicz & Delfs, 1990b; Capecchi & Vestroni, 1995; Mahla & Badan Palhares, 1993] etc.

Mathematical results are sometimes available for studying existence and uniqueness of such nonlinear dynamical systems [Brezis, 1973; Schatzman, 1978; Deimling, 1992; Monteiro Marques, 1994; Moreau, 1988], but generally such results are not followed by correct numerical investigations if the exact integration of the nonlinear system is not possible (a correct mathematical frame work is given in for example [Paoli, 1993; Paoli & Schatzman, 1993]).

Our intention here is to generalize the Chua double scroll model to a kind of "unsmooth" paradigm. In Sec. 2, we introduce a model with a finite number of discontinuities. In Sec. 3, we describe the mechanical point of view. In Sec. 4, we present the mathematical frame, study existence and uniqueness of solutions in the general case, and

apply the previous results to particular cases of discontinuities (at zero, and both -1 and 1). In Sec. 5, we show how to analytically build the solutions for the two previous cases. In Sec. 6, we present numerical results for two particular cases. In the first case two discontinuities at -1 and 1 are considered: Bifurcation diagrams are presented and transition to chaos via a bifurcation cascade is investigated. In the second case, discontinuity is located at 0. Bifurcation diagrams are illustrated by phase portraits, Poincaré sections and global behavior. Trapping areas for the trivial equilibrium are studied. Chaos is pointed out by using the computation of Lyapunov exponents. Then in the last section we draw conclusions from our work and point out some extensions.

2. Generalized Double Scroll Chua Circuit

Let us introduce Chua's system and its generalization. Chua's system is a paradigm [Madan, 1993]. It is related to the behavior of an electrical circuit possessing a diode with a nonlinear response [Chua *et al.*, 1986; Komuro *et al.*, 1991]. It is a system of three differential equations of first order usually written as

$$\begin{cases} \dot{X} = \alpha(Y - h(X)) \\ \dot{Y} = X - Y + Z \\ \dot{Z} = -\beta Y \end{cases} \tag{1}$$

with α and β two positive parameters, and $h : \mathbb{R} \to \mathbb{R}$ concentrates the nonlinearities. This system can be given in the form

$$\dot{y} = \mathcal{L}y - \alpha H(y) \tag{2}$$

with

$$y = \begin{pmatrix} X \\ Y \\ Z \end{pmatrix}, \quad \mathcal{L} = \begin{pmatrix} 0 & \alpha & 0 \\ 1 & -1 & 1 \\ 0 & -\beta & 0 \end{pmatrix}, \quad H\begin{pmatrix} X \\ Y \\ Z \end{pmatrix} = \begin{pmatrix} h(X) \\ 0 \\ 0 \end{pmatrix} \tag{3}$$

so that we distinguish the linear part from the nonlinear one. The function h is a piecewise-linear function that is expressed as follows:

$$h(X) = \begin{cases} m_1 X + (m_0 - m_1) & \text{if } X \geq 1 \\ m_0 X & \text{if } |X| \leq 1 \\ m_1 X - (m_0 - m_1) & \text{if } X \leq -1 \end{cases} \tag{4}$$

with $m_0 < 0$ and $m_1 > 0$. Here we consider generalizations of Chua's circuit by introducing discontinuities in the frame of multivalued differential equations. In the previous classical Chua circuit, we only modify function h. The system we are dealing with is written as

$$\begin{cases} \dot{X} = \alpha(Y - \delta(X)) \\ \dot{Y} = X - Y + Z \\ \dot{Z} = -\beta Y \end{cases} \tag{5}$$

where $\delta(X) = l(X) + m(X)$. Function l denotes a piecewise-linear continuous function and m denotes a function with a finite number N of discontinuities. Indeed, at every point of discontinuity X_j, $j = 1, \ldots, N$ we assume that $m(X_j) = [m(X_j^-); m(X_j^+)]$ with

$$\lim_{\substack{X \to X_j \\ X < X_j}} m(X) = m(X_j^-)$$

and

$$\lim_{\substack{X \to X_j \\ X > X_j}} m(X) = m(X_j^+) \text{ (and } m(X_j^+) > m(X_j^-))$$

Thus we obtain a new differential equation (or rather differential inclusion) of the form

$$\dot{y} - \mathcal{L}y + \alpha\Delta(y) \ni 0 \tag{6}$$

with

$$\Delta : \begin{cases} \mathbb{R}^3 \to \mathbb{R}^3 \\ \begin{pmatrix} X \\ Y \\ Z \end{pmatrix} \mapsto \begin{pmatrix} \delta(X) \\ 0 \\ 0 \end{pmatrix} \end{cases} \tag{7}$$

and $\Delta = L + M$ where

$$L : \begin{cases} \mathbb{R}^3 \to \mathbb{R}^3 \\ \begin{pmatrix} X \\ Y \\ Z \end{pmatrix} \mapsto \begin{pmatrix} l(X) \\ 0 \\ 0 \end{pmatrix} \end{cases}$$
$$M : \begin{cases} \mathbb{R}^3 \to \mathbb{R}^3 \\ \begin{pmatrix} X \\ Y \\ Z \end{pmatrix} \mapsto \begin{pmatrix} m(X) \\ 0 \\ 0 \end{pmatrix} \end{cases} \tag{8}$$

For the numerical study, we deal with two particular cases: First a symmetric discontinuity both in -1 and 1 added to the classical Chua system, and

second a single discontinuity in 0 similarly added to the Chua system. The first case corresponds to

$$l = h \quad m(X) = \begin{cases} -\varepsilon & \text{if } X < -1 \\ 0 & \text{if } -1 < X < 1 \\ \varepsilon & \text{if } 1 < X \end{cases} \tag{9}$$

The second case corresponds to

$$l(X) = \begin{cases} m_1 X + m_0 - m_1 - 2\varepsilon & \text{if } X \geq 1 \\ (m_0 - \varepsilon)X - \varepsilon & \text{if } -1 \leq X \leq 1 \\ m_1 X - m_0 + m_1 & \text{if } X \leq -1 \end{cases} \tag{10}$$

and the discontinuous function m is defined by

$$m(X) = \begin{cases} 0 & \text{if } X < 0 \\ 2\varepsilon & \text{if } X > 0 \end{cases} \tag{11}$$

It can be noticed that in the case of discontinuity at 0, the slopes of the initial "unperturbed" Chua circuit are modified. But in the case of discontinuity at -1 and 1 these initial slopes remain unchanged.

3. Mechanical Point of View

Let us show that the Chua circuit corresponds to a special mechanical system with a particular nonlinear constitutive law. Let us consider the following one degree of freedom mechanical system:

$$m\ddot{w} + g\dot{w} + kw = -\tau(w, \dot{w}) \tag{12}$$

Note that $[m] = kg$, $[g] = Ns$, $[\tau] = Nm^{-1}$ and that w is a nondimensional deformation. Assume that

$$\tau(w, \dot{w}) = \tau_0 \Psi(S)$$

where $[\tau_0] = Nm^{-1}$ and $\Psi(S)$ is nondimensional of the form

$$\Psi(S) = \begin{cases} (1+F)S + E - F - \Omega & \text{for } S \geq 1 \\ (1+E)S - \Omega & \text{for } 0 < S \leq 1 \\ (1+E)S + \Omega & \text{for } -1 \leq S < 0 \\ (1+F)S - E + F + \Omega & \text{for } S \geq 1 \end{cases} \tag{13}$$

where E, F and Ω are nondimensional. $S(w, \dot{w})$ is a nondimensional form of the tension

$$S = \frac{\tau_1}{\tau_0} + \frac{\tau_2}{\tau_0} + \frac{\tau_3}{\tau_0}$$

where

$$\tau_1 = a_1' w \quad \tau_2 = a_2' \dot{w} \quad \tau_3 = b_1' \int_0^t w(e)de$$

Thus we have

$$S(w, \dot{w}) = a_1 w + a_2 \dot{w} + b_1 \int_0^t w(e)de$$

where

$$a_1 = \frac{a_1'}{\tau_0} \quad a_2 = \frac{a_2'}{\tau_0} \quad b_1 = \frac{b_1'}{\tau_0}$$

and $[a_1]$ nondimensional, $[a_2] = s$, $[b_1] = s^{-1}$. After introducing the nondimensional time $q = \sqrt{(k/m)}t$, we get

$$S\left(w, \frac{dw}{dq}\right) = a_1 w + a_2 \sqrt{\frac{k}{m}} \frac{dw}{dq} + \nu_2 \int_0^q w(e)de \tag{14}$$

Setting

$$a_1 = 1\,, \quad a_2 \sqrt{\frac{k}{m}} = 1\,, \quad \nu_2 = \frac{b_1}{\sqrt{\frac{k}{m}}}$$

$$E = a\,, \quad F = b\,, \quad \Omega = c$$

we obtain function ψ of Chua's equations:

$$\psi(r) = \begin{cases} (1+b)r + a - b - c & r \geq 1 \\ (1+a)r - c & 0 < r \leq 1 \\ (1+a)r + c & -1 < r \leq 0 \\ (1+b)r - a + b + c & r \leq -1 \end{cases}$$

Our "rheological" nondimensional equation

$$m\left(\sqrt{\frac{k}{m}}\right)^2 \frac{d^2 w}{dq^2} + g\sqrt{\frac{k}{m}} \frac{dw}{dq} + kw = -\tau_0 \Psi(S) \tag{15}$$

corresponds to Chua's equation

$$\ddot{z} + \dot{z} + (\nu_2 - \nu_1)z = -\nu_1 \psi(\tilde{z}) \tag{16}$$

with $\dot{\tilde{z}} = z$. Comparing (15) and (16) we get

$$\frac{m\sqrt{\frac{k}{m}}}{g} = 1\,, \quad \frac{k}{\sqrt{\frac{k}{m}}g} = \nu_1 - \nu_2\,, \quad \frac{\tau_0}{\sqrt{\frac{k}{m}}g} = \nu_1$$

which leads to the equation

$$k = \tau_0 - g b_1\,.$$

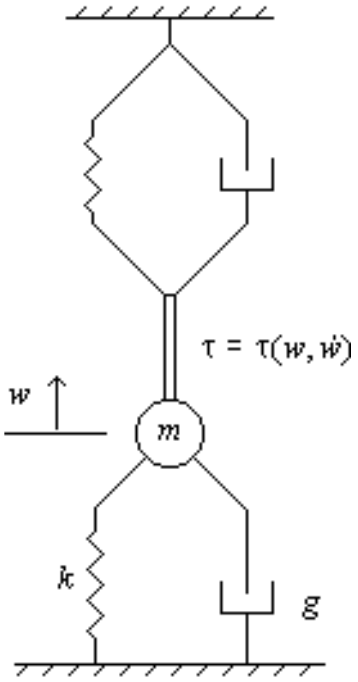

Fig. 1. Rheological model corresponding to Chua circuit.

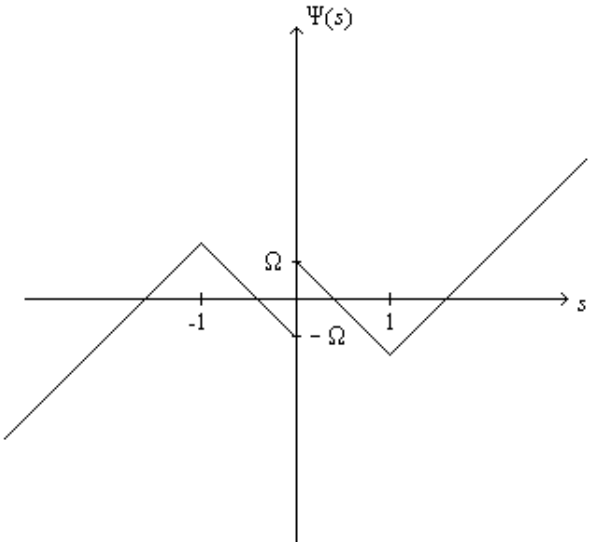

Fig. 2. Piecewise-linear characteristic $\Psi(s)$.

This mechanical system is described in Fig. 1 and corresponds to the piecewise-linear characteristic $\Psi(s)$ presented in Fig. 2.

We have introduced several parameters in order to describe our mechanical model. In the next sections, we deal with the Chua circuit. This Chua circuit is defined by several parameters: α, β, m_0, m_1, ε. Indeed the occurrence of the following relations allows us to transform our mechanical model into a Chua circuit:

$$\alpha=\nu_1\,,\ \beta=\nu_2\,,\ \varepsilon=-c\,,\ m_1=1+b\,,\ m_0=1+a-c\,.$$

4. Existence and Uniqueness of Solutions

4.1. *Usual Chua's system*

Let $T \in \mathbb{R}^{+\star}$ and $\Omega = [0, T]$. Let us consider the following ordinary differential equation

$$\begin{cases} \dot{y}(t) = \mathcal{L}y(t) - \alpha H(y(t)) = f(t, y(t)) \quad \forall t \in]0, T] \\ y(0) = y_0 \in \mathbb{R}^3 \end{cases} \tag{17}$$

Here $f \in C^0(\Omega \times \mathbb{R}^3)$ because $\mathcal{L}$ is linear and H continuous. Moreover, h is piecewise-linear and then Lipschitz-continuous with Lipschitz constant

$$K = \max(m_1 - 2m_0,\, 2m_1 - m_0)\,.$$

So f is Lipschitz continuous with Lipschitz constant

$$L = \sqrt{\max(3 + 2\alpha^2K^2,\, 3 + 2\alpha^2 + \beta^2)}\,.$$

The system of Eqs. (17) verifies assumptions of the Cauchy–Lipschitz theorem that provides existence and uniqueness of the solution of this system for every T.

4.2. *Mathematical background: Maximal monotonous operators*

Let us recall some useful results that will be used to prove existence and uniqueness of solutions of the generalized Chua system.

Let H be a real Hilbert space with scalar product $(.,.)$ and norm $\|\cdot\|$.

Definition 1. A multivalued operator A on H is a map from H to $\mathcal{P}(H)$ the set of the subsets of H. Let us define $D(A) = \{x \in H,\, Ax \neq \emptyset\}$. $D(A)$ is called the domain of A.

An operator A is identified to its graph in $H \times H$ that is defined by

$$\{(x,\, y),\, x \in H,\, y \in Hx\}\,.$$

Definition 2. An operator A on H is monotonous iff

$$\forall x_1,\, x_2 \in D(A) \quad (Ax_1 - Ax_2,\, x_1 - x_2) \geq 0$$

or exactly

$$\forall x_1,\, x_2 \in D(A) \quad \forall y_1 \in Ax_1 \quad \forall y_2 \in Ax_2$$
$$(y_1 - y_2,\, x_1 - x_2) \geq 0\,.$$

It can be seen that if A is singlevalued this last definition actually means that A is increasing. So a simple example of monotonous operator on $\mathbb{R}$ is given by

$$\tilde{f} : \begin{cases} \mathbb{R} \to \mathcal{P}(\mathbb{R}) \\ x \mapsto [f(x^-),\, f(x^+)] \cap \mathbb{R} \end{cases}$$

with $f : \mathbb{R} \to \mathbb{R}$ an increasing function.

Definition 3. An operator on H is said to be maximal monotonous iff it is maximal in the set of the monotonous operators on H.

One can notice that "maximal" here refers to the inclusion of graphs: For two operators A and B, $A \subset B$ iff $\forall x \in H$, $Ax \subset Bx$.

Now let us recall some properties and theorems that give existence and uniqueness results in the cases we are dealing with. Proofs and details can be found in [Brezis, 1973]. Understanding of multivalued differential equations can be found in [Deimling, 1992].

Theorem 1. *Let A be a maximal monotonous operator. Let $D(B)$ be a convex subset of H and B a semi-continuous monotonous singlevalued operator from $D(B)$ to H. Let us assume that $D(A) \subset D(B)$ and that there exists $k < 1$ and θ a continuous function so that $\forall x \in D(A)$, $\|Bx\| \leq k\|A^0 x\| + \theta(\|x\|)$ where $A^0 x$ is equal to the projection of 0 onto Ax (we write $A^0 x = \mathrm{Proj}_{Ax} 0$). Then $A + B$ is a maximal monotonous operator.*

Let us recall results that link the theory of maximal monotonous operators to ordinary differential equations.

Theorem 2. *Let A be a maximal monotonous operator with domain $D(A)$. For all $u_0 \in D(A)$, there exists a unique function $u : [0, +\infty[\to H$ which verifies*:

(1) $\forall t > 0 \quad u(t) \in D(A)$
(2) *u is Lipschitz continuous on $[0, +\infty[$ and $\|du/dt\|_{L^\infty([0,+\infty[,H)} \leq \|A^0 u_0\|$*
(3) $(du/dt)(t) + Au(t) \ni 0$
(4) $u(0) = u_0$
(5) *at any $t \in [0, +\infty[$, u possesses a right derivative and we have*

$$\forall t \in [0, +\infty[\quad \frac{d^+ u}{dt}(t) + A^0 u(t) = 0\,.$$

Property (5) is very important because it is verified everywhere whereas relationship (3) is only verified almost everywhere.

Theorem 3. *Let A be a maximal monotonous operator with domain $D(A)$. Then for every $f \in L^1([0, T], H)$ and every $u_0 \in \overline{D(A)}$, there exists a unique weak solution u of the equation $(du/dt) + Au \ni f$ verifying $u(0) = u_0$.*

In order to obtain a result similar to property (5) of Theorem 2, some assumptions have to be added. We have:

Theorem 4. *Let A be a maximal monotonous operator of H, $f \in L^1([0, T], H)$ and let $u \in C([0, T], H)$ be a weak solution of equation $(du/dt) + Au \ni f$. Let $t_0 \in [0, T[$ a right Lebesgue point of f (resp. $t_0 \in]0, T[$ a Lebesgue point of f). Let us set*

$$f(t_0 + 0) = \lim_{h \searrow 0} \frac{1}{h} \int_{t_0}^{t_0 + h} f(s)ds$$

Then the following properties are equivalent:

(i) $u(t_0) \in D(A)$
(ii) $\liminf_{h \searrow 0} (1/h)|u(t_0 + h) - u(t_0)| < +\infty$ (*resp.* $\liminf_{\substack{h \to 0 \\ h \neq 0}} (1/h)|u(t_0 + h) - u(t_0)| < +\infty$)
(iii) *u has a right derivative at t_0 and $(d^+ u/dt)(t_0) = f(t_0 + 0) - \mathrm{Proj}_{Au(t_0)} f(t_0 + 0)$*

The next result leads to a strong solution under convenient assumptions.

Theorem 5. *Let H be a finite dimensional Hilbert space. Let A be a maximal monotonous operator so that $\mathrm{Int}(D(A)) \neq \emptyset$. Let f belong to $L^1([0, T], H)$. Then every weak solution of the equation $(du/dt) + Au \ni f$ is a strong solution.*

Indeed a strong solution is a function $u \in C([0, T], H)$ absolutely continuous on every

compact subset of $]0, T[$ verifying:

$$u(t) \in D(A) \quad \text{and almost everywhere in} \quad]0, T[$$
$$\frac{du}{dt}(t) + Au(t) \ni f$$

A function $u \in C([0, T], H)$ is a weak solution if and only if there exists series $f_n \in L^1([0, T], H)$ and $u_n \in C([0, T], H)$ so that u_n is a strong solution of equation $(du_n/dt)(t) + Au_n(t) \ni f_n(t)$, with $\lim_{n\to+\infty} f_n = f$ in $L^1([0, T], H)$ and uniformly on $[0, T]$: $\lim_{n\to+\infty} u_n = u$.

Hence it can be seen that if $f \in L^1([0, T])$, u is a strong solution iff u is a weak solution and u is absolutely continuous on every compact subset of $]0, T[$.

Theorem 6. [Brezis, 1973, p. 105]. *Let A be a maximal monotonous operator on H. Let us choose $\omega > 0$, $f \in L^1([0, T], H)$ and $u_0 \in \overline{D(A)}$. Then there is a unique weak solution of the equation*

$$\begin{cases} \dfrac{du}{dt}(t) + Au(t) - \omega u(t) \ni f \\ u(0) = u_0 \end{cases}$$

One can derive from Theorem 5 and from the proof of Theorem 6 that if $\dim(H) < +\infty$ and $\mathrm{Int}(D(A)) \neq \emptyset$ then the weak solution of Theorem 6 is a strong solution.

4.3. *Existence and uniqueness for the generalized Chua circuit*

The Usual Cauchy–Lipschitz theorem does not work in the generalized case. It is not possible to use the theorem of Caratheodory (see [Crouzeix & Mignot, 1974]) either, which possesses assumptions weaker than the assumptions of the Cauchy–Lipschitz theorem. We apply the results of the theory of maximal monotonous operators to the generalized Chua system. Let us consider the following problem:

$$\begin{cases} \dot{y} = \mathcal{L}y - \alpha M(y) - \alpha L(y) \\ y(0) = y_0 \end{cases} \tag{18}$$

where $\mathcal{L}$ is defined in Sec. 1, M denotes a maximal monotonous operator on $\mathbb{R}^3$ and L a Lipschitz continuous map of $\mathbb{R}^3$. The following claim provides existence and uniqueness of the solution for a system even more general than system (18).

Theorem 7. *Let A be a maximal monotonous operator on $\mathbb{R}^3$ and F a Lipschitz continuous function on $\mathbb{R}^3$. Then system (19) has a unique strong solution on $[0, T]$ for every $T > 0$ where:*

$$\begin{cases} \dot{y} + Ay + Fy \ni 0 \\ y(0) = y_0 \end{cases} \tag{19}$$

Moreover, we have:

$$\forall t_0 \in [0, T], \ \frac{dy^+}{dt}(t_0) = -\mathrm{Proj}_{(A+F)y(t_0)}(0)\,. \tag{20}$$

The proof is obtained by using Theorem 6. Let us define the Lipschitz continuous operator G on $\mathbb{R}^3$ as follows: $G(y) = F(y) - F(0)$ and let us set $f \equiv -F(0)$. Now system (19) is equivalent to (21):

$$\begin{cases} \dot{y} + Ay + Gy \ni f \\ y(0) = y_0 \end{cases} \tag{21}$$

Assumptions of Theorem 5 are verified ($f \in L^1([0, T], \mathbb{R}^3)$ and $\mathbb{R}^3$ is a Hilbert space of finite dimension!). Moreover every $t_0 \in [0, T]$ is a Lebesgue point here because f is constant. So we apply Theorem 4 to the weak solutions we have just obtained.

Let p be the Lipschitz constant of F. G has the same Lipschitz constant. By assumption $G(0) = 0$, hence we have:

$$\forall x \in \mathbb{R}^3 \quad \|G(x)\| \leq p\|x\| \tag{22}$$

Let us set $B = G + pI$. We have

$$\forall x \in \mathbb{R}^3 \quad \|Bx\| \leq \|G(x)\| + p\|x\| \tag{23}$$

and then

$$\forall x \in \mathbb{R}^3 \quad \|Bx\| \leq 2p\|x\| \tag{24}$$

B is a monotonous operator: for x_1, $x_2 \in \mathbb{R}^3$ we see that

$$(Bx_1 - Bx_2,\, x_1 - x_2) = (G(x_1) - G(x_2),\, x_1 - x_2) + p\|x_1 - x_2\|^2\,. \tag{25}$$

Because

$$\begin{aligned} &|(G(x_1) - G(x_2),\, x_1 - x_2)| \\ &\quad \leq \|G(x_1) - G(x_2)\|\,\|x_1 - x_2\| \\ &\quad \leq p\|x_1 - x_2\|^2 \end{aligned} \tag{26}$$

we get

$$(G(x_1) - G(x_2),\, x_1 - x_2) + p\|x_1 - x_2\|^2 \geq 0 \tag{27}$$

and B is monotonous. We apply Theorem 1, here with $D(A) = D(B) = H = \mathbb{R}^3$, $k = 0$ and the continuous function θ is defined by

$$\theta : \begin{cases} \mathbb{R}^+ \to \mathbb{R}^+ \\ x \mapsto 2px \end{cases} \tag{28}$$

We obtain $A + B$ maximal monotonous so $A + G + pI = A_1$ is maximal monotonous. Now we apply Theorem 6 to A_1 and $\omega = p$. There is a unique weak solution of

$$\begin{cases} \dot{y} + A_1 y - py \ni 0 \\ y(0) = y_0 \end{cases} \tag{29}$$

which is indeed a strong solution.

We have

$$\frac{dy^+}{dt}(t_0) = f(t_0^+) + py(t_0^+) - \mathrm{Proj}_{A_1 y(t_0)}(f(t_0^+) + py(t_0^+)) \tag{30}$$

Because of the equalities $A_1 = A + G + pI = A + F - F(0) + pI$ and $f \equiv F(0)$, we express the previous relationship in the form:

$$\begin{aligned} \frac{dy^+}{dt}(t_0) &= -F(0) + py(t_0) \\ &\quad - \mathrm{Proj}_{(A+F)y(t_0) - F(0) + py(t_0)} \\ &\qquad (-F(0) + py(t_0)) \\ &= -\mathrm{Proj}_{(A+F)y(t_0)}(0) \end{aligned} \tag{31}$$

Now we can affirm that the problem

$$\begin{cases} \dot{y} + Ay + Fy \ni 0 \\ y(0) = y_0 \end{cases}$$

has a unique strong solution on $[0, T]$, $\forall T > 0$. This solution verifies:

$$\forall t_0 \in [0, T],\ \frac{dy^+}{dt}(t_0) = -\mathrm{Proj}_{(A+F)y(t_0)}(0)\,. \tag{32}$$

We have just proved existence and uniqueness of the solution of system (18).

One can note that indeed we have proved existence and uniqueness of the solution of any problem of the kind of system (18) submitted to a Lipschitz continuous perturbation.

It is clear that because the solution obtained is continuous, (18) provides Y and Z in $C^1(\mathbb{R}^+)$ and X only C^1-piecewise because defects of continuity of $\dot{X}$ occur at times t when $X(t)$ is a point of discontinuity of function m.

4.4. *Applications to two particular cases*

4.4.1. *Chua's system with discontinuities at -1 and 1*

We deal with the system

$$\begin{cases} \dot{X} = \alpha(Y - \delta(X)) \\ \dot{Y} = X - Y + Z \\ \dot{Z} = -\beta Y \end{cases} \tag{33}$$

with $\delta(X) = h(X) + m(X)$. m can be written in the following form

$$m(X) = \begin{cases} \{-\varepsilon\} & \text{if } X < -1 \\ [-\varepsilon,\, 0] & \text{if } X = -1 \\ \{0\} & \text{if } -1 < X < 1 \\ [0,\, \varepsilon] & \text{if } X = 1 \\ \{\varepsilon\} & \text{if } X > 1 \end{cases} \tag{34}$$

so that it is a multivalued operator. We assume that $0 \le \varepsilon \le -m_0$.

Thus we deal with the system

$$\dot{y} - (\mathcal{L} - \alpha H)y + \alpha M y \ni 0 \tag{35}$$

where operator $-(\mathcal{L} - \alpha H)$ is Lipschitz continuous on $\mathbb{R}^3$. It is clear that M is monotonous iff

$$\forall X_1,\, X_2 \in \mathbb{R}, \quad (m(X_1) - m(X_2),\, X_1 - X_2) \ge 0\,.$$

We can assume for instance that $X_1 < X_2$. Then M is monotonous iff

$$\forall S_1 \in m(X_1),\, \forall S_2 \in m(X_2), \quad S_1 - S_2 \le 0\,.$$

We can distinguish between five cases: $X_1 \in]-\infty, -1[$, $X_1 = -1$, $X_1 \in]-1, 1[$, $X_1 = 1$, $X_1 \in]1, +\infty[$. Let us discuss the first one for example, the four other cases being similar. If $X_1 \in]-\infty, -1[$, we have $m(X_1) = \{-\varepsilon\}$. And

$$\forall X \in \mathbb{R}, \quad m(X) \in [-\varepsilon,\, \varepsilon] \to \forall S_2 \in m(X_2),\ S_2 \ge -\varepsilon$$

Then it is clear that in this case $m(X_1) - m(X_2) \le 0$.

Moreover it is easy to see that M is maximal. We have $\mathrm{Im}(I + M) = \mathbb{R}^3 = H$. Theorem 3.2 of [Brézis, 1973] provides Δ maximal monotonous. Because $\alpha > 0$, αM is maximal monotonous too.

Thus system (35) verifies all the assumptions of Theorem 7. It possesses a unique strong solution on $[0, T]$ for every $T > 0$.

It is convenient to apply the second part of this theorem to obtain the value of $\dot{y}$ at the crossing of $X = 1$. For t_0 so that $X(t_0) = 1$ we get:

$$\frac{dy^+}{dt}(t_0) = -\mathrm{Proj}_{(\alpha M - \mathcal{L} + \alpha H)y(t_0)}(0) = \begin{pmatrix} S \\ U \\ V \end{pmatrix} \in (-\alpha M + \mathcal{L} - \alpha H)y(t_0) \quad (36)$$

Let us set

$$y(t_0) = \begin{pmatrix} 1 \\ Y \\ Z \end{pmatrix} \quad (37)$$

We have

$$\mathcal{L}y(t_0) = \begin{pmatrix} \alpha Y \\ 1 - Y + Z \\ -\beta Y \end{pmatrix} \qquad \alpha M y(t_0) = \begin{pmatrix} \alpha m(1) \\ 0 \\ 0 \end{pmatrix} \quad (38)$$

$$Hy(t_0) = \begin{pmatrix} h(1) \\ 0 \\ 0 \end{pmatrix} = \begin{pmatrix} m_0 \\ 0 \\ 0 \end{pmatrix} \quad (39)$$

and then

$$\begin{pmatrix} S - \alpha Y + \alpha m_0 \\ U - 1 + Y - Z \\ V + \beta Y \end{pmatrix} \in -\alpha \begin{pmatrix} [0,\, \varepsilon] \\ \{0\} \\ \{0\} \end{pmatrix} \quad (40)$$

that yields

$$\begin{pmatrix} \alpha(Y - m_0 - \varepsilon) \le S \le \alpha(Y - m_0) \\ U = 1 - Y + Z \\ V = -\beta Y \end{pmatrix} \quad (41)$$

Because of the definition of the projection, $(S, U, V)^t$ has the smallest norm. Here this means that x^2 has to be minimal. We distinguish between three cases:

— if $Y < m_0$, $\min_{\alpha(Y-m_0-\varepsilon)\le S\le\alpha(Y-m_0)} S^2$ corresponds to $S = \alpha(Y - m_0)$. So we obtain

$$\frac{dy^+}{dt}(t_0) = \begin{pmatrix} \alpha(Y(t_0) - m_0) \\ 1 - Y(t_0) + Z(t_0) \\ -\beta Y(t_0) \end{pmatrix} \quad (42)$$

— if $Y > m_0 + \varepsilon$, $\min_{\alpha(Y-m_0-\varepsilon)\le S\le\alpha(Y-m_0)} S^2$ corresponds to $S = \alpha(Y - m_0 - \varepsilon)$. So we obtain

$$\frac{dy^+}{dt}(t_0) = \begin{pmatrix} \alpha(Y(t_0) - m_0 - \varepsilon) \\ 1 - Y(t_0) + Z(t_0) \\ -\beta Y(t_0) \end{pmatrix} \quad (43)$$

— if $m_0 \le Y \le m_0 + \varepsilon$, $\min_{\alpha(Y-m_0-\varepsilon)\le S\le\alpha(Y-m_0)} S^2$ corresponds to $S = 0$. So we obtain

$$\frac{dy^+}{dt}(t_0) = \begin{pmatrix} 0 \\ 1 - Y(t_0) + Z(t_0) \\ -\beta Y(t_0) \end{pmatrix} \quad (44)$$

It can be noticed that the values $\dot{Y}(t_0^+)$ and $\dot{Z}(t_0^+)$ provided by this procedure can be direcly derived from system (33).

It is necessary to assume that $\alpha > 0$ in order to apply this method.

Note. One can think of other methods to prove existence and uniqueness results. For example it would be possible to smooth the discontinuity by using piecewise-linear continuous functions or C^∞ functions. But it seems difficult to have *a priori* estimations that allow to control the limits in the smooth systems of differential equations.

Another method is to take into account the particular form of the system. It deals with joining pieces of solutions of linear system of differential equations. The difficulty is to write the crossing of discontinuity plane in order to obtain piecewise C^1 solutions. In our cases this method is available. But it is clear that if we slightly modify the Lipschitz continuous part (small smooth perturbations so that explicit calculation of solutions is not possible), it becomes necessary to use the theory of maximal monotonous operators.

4.4.2. *Chua's system with discontinuity at* 0

In this case the starting system of equations is

$$\begin{cases} \dot{X} = \alpha(Y - \delta(X)) \\ \dot{Y} = X - Y + Z \\ \dot{Z} = -\beta Y \end{cases} \quad (45)$$

where $\delta(x) = l(x) + m(x)$ (see Sec. 2). The multivalued function m is defined according to

$$m(x) = \begin{cases} \{0\} & \text{if } x < 0 \\ [0,\, 2\varepsilon] & \text{if } x = 0 \\ \{2\varepsilon\} & \text{if } x > 0 \end{cases} \quad (46)$$

We write again this system in the form

$$\dot{y} - (\mathcal{L} - \alpha L)y + \alpha M y \ni 0 \tag{47}$$

Because $\mathcal{L}$ is linear and then is Lipschitz continuous, and L is Lipschitz continuous (l is piecewise-linear), operator $-(\mathcal{L} - \alpha L)$ is Lipschitz continuous on $\mathbb{R}^3$.

It is easy to prove that M is monotonous: This is similar to the previous case. As we did in the previous subsection for the first example, we deduce that αM is a maximal monotonous operator.

It is clear that assumptions of Theorem 7 are verified by system (45): It possesses a unique strong solution on $[0, T]$ for every $T > 0$.

Moreover, let us pay attention to the second part of the result of Theorem 7 and calculate $\dot{y}$ at $X = 0$ crossing. For t_0 so that $X(t_0) = 0$ we have

$$\begin{aligned}\frac{dy^+}{dt}(t_0) &= -\mathrm{Proj}_{(\alpha M - \mathcal{L} + \alpha L)y(t_0)}(0) \\ &= \begin{pmatrix} S \\ U \\ V \end{pmatrix} \in (\mathcal{L} - \alpha M - \alpha L)y(t_0)\end{aligned} \tag{48}$$

Let us set

$$y(t_0) = \begin{pmatrix} 0 \\ Y \\ Z \end{pmatrix} \tag{49}$$

We have

$$\mathcal{L}y(t_0) = \begin{pmatrix} \alpha Y \\ -Y + Z \\ -\beta Y \end{pmatrix},\ \alpha M y(t_0) = \begin{pmatrix} m(0) \\ 0 \\ 0 \end{pmatrix} \tag{50}$$

$$L y(t_0) = \begin{pmatrix} l(0) \\ 0 \\ 0 \end{pmatrix} = \begin{pmatrix} -\varepsilon \\ 0 \\ 0 \end{pmatrix} \tag{51}$$

Hence we obtain

$$\begin{pmatrix} S - \alpha Y - \alpha\varepsilon \\ U + Y - Z \\ V + \beta Y \end{pmatrix} \in -\alpha \begin{pmatrix} [0,\, 2\varepsilon] \\ \{0\} \\ \{0\} \end{pmatrix} \tag{52}$$

that yields

$$\begin{cases} \alpha(Y - \varepsilon) \le S \le \alpha(Y + \varepsilon) \\ U = -Y + Z \\ V = -\beta Y \end{cases} \tag{53}$$

Because of the definition of the projection, the solution $(S, U, V)^t$ has the smallest norm i.e. again S^2 has to be the smallest.

We can divide the calculation into three cases:

— if $Y < -\varepsilon$, $\min_{\alpha(Y-\varepsilon) \le S \le \alpha(Y+\varepsilon)} S^2$ corresponds to $S = \alpha(Y + \varepsilon)$. Hence we get

$$\frac{dy^+}{dt}(t_0) = \begin{pmatrix} \alpha(Y(t_0) + \varepsilon) \\ -Y(t_0) + Z(t_0) \\ -\beta Y(t_0) \end{pmatrix} \tag{54}$$

— if $Y > \varepsilon$, $\min_{\alpha(Y-\varepsilon) \le S \le \alpha(Y+\varepsilon)} S^2$ corresponds to $S = \alpha(Y - \varepsilon)$. Hence we get

$$\frac{dy^+}{dt}(t_0) = \begin{pmatrix} \alpha(Y(t_0) - \varepsilon) \\ -Y(t_0) + Z(t_0) \\ -\beta Y(t_0) \end{pmatrix} \tag{55}$$

— if $-\varepsilon \le Y \le \varepsilon$, $\min_{\alpha(Y-\varepsilon) \le S \le \alpha(Y+\varepsilon)} S^2$ corresponds to $S = 0$. Hence we get

$$\frac{dy^+}{dt}(t_0) = \begin{pmatrix} 0 \\ -Y(t_0) + Z(t_0) \\ -\beta Y(t_0) \end{pmatrix} \tag{56}$$

5. Analytical Calculation of the Solution

We build analytical solutions for the two particular cases that we have considered in the previous section from the point of view of existence and uniqueness.

5.1. *Discontinuity crossing*

5.1.1. *Case 1: Discontinuity at* -1 *and* 1

Because of the symmetry of the system of Eqs. (33) it is sufficient to study the case $X = 1$. Let us set $D_1 =]1, +\infty[\times \mathbb{R}^2$ and $D_0 =]-1, 1[\times \mathbb{R}^2$.

We determine the necessary conditions of crossing into the different areas D_0, D_1 and $X = 1$. Let us assume that for a given t_0 we have $X(t_0) = 1$. One can already notice that if $Y < m_0$ or $Y > m_0 + \varepsilon$, then we can conclude from (42) and (43).

(1) *The trajectory runs into* D_1:

In this case one has $X(t_0^+) > 1$ and X is locally increasing after t_0 that yields $\dot{X}(t_0 + \eta) > 0$ for η small enough. We get $\dot{X}(t_0 + \eta) = \alpha(Y(t_0 + \eta) - \delta(X(t_0 + \eta))) > 0$. Because of continuity of X and Y we write

$$Y(t_0 + \eta) \underset{\eta \searrow 0}{\longrightarrow} Y(t_0) \quad X(t_0 + \eta) \underset{\eta \searrow 0}{\searrow} 1$$

and then

$$\delta(X(t_0+\eta)) \underset{\eta \searrow 0}{\longrightarrow} m_0+\varepsilon$$

So we get $Y(t_0) \geq m_0+\varepsilon$.

(2) *The trajectory runs into D_0*:

Here we have $X(t_0^+) < 1$ and X is locally decreasing after t_0 that yields $\dot{X}(t_0+\eta) < 0$ for η small enough. We get $\dot{X}(t_0+\eta) = \alpha(Y(t_0+\eta) - \delta(X(t_0+\eta))) < 0$. Because of continuity of X and Y we write

$$Y(t_0+\eta) \underset{\eta \searrow 0}{\longrightarrow} Y(t_0) \quad X(t_0+\eta) \underset{\eta \searrow 0}{\nearrow} 1$$

and then

$$\delta(X(t_0+\eta)) \underset{\eta \searrow 0}{\longrightarrow} m_0$$

So we get $Y(t_0) \leq m_0$.

(3) *Trajectory runs into $X = 1$*:

X is constant and C^1 on an open set of nonzero measure. Consequently we have $\dot{X} = 0$ on this open set, hence $Y(t) \in \delta(1) = [m_0,\, m_0+\varepsilon]$. So the trajectory stays in $X = 1$ as long as we have $Y(t) \in [m_0,\, m_0+\varepsilon]$.

Two cases have to be taken into account: $Y(t_0) = m_0$ and $Y(t_0) = m_0+\varepsilon$.

(a) If $Y(t_0) = m_0$, the trajectory can either stay in $X = 1$ or go into D_0. In order that it stays in $X = 1$ we need $\dot{X}(t_0+\eta) = 0$ for $\eta > 0$ small enough, hence from (33) $Y(t_0+\eta) \in \delta(X(t_0+\eta)) = \delta(1) = [m_0,\, m_0+\varepsilon]$. The latter leads to $Y(t_0+\eta) \geq Y(t_0)$ and then $\dot{Y}(t_0) \geq 0$. This inequality provides a condition for Z coordinate: $Z(t_0) \geq m_0 - 1$.

Let us look for a necessary condition of passing into D_0. We have $\dot{X}(t_0^+) = 0$. Let us calculate $\ddot{X}(t_0^+)$. One has $\ddot{X}(t_0^+) = \alpha(\dot{Y}(t_0) - m_0\dot{X}(t_0^+))$. We conclude that $\ddot{X}(t_0^+) = \alpha(1 - m_0 + Z(t_0))$. It is necessary to have $\dot{X}(t_0+\eta) < 0 = \dot{X}(t_0^+)$ so $\ddot{X}(t_0^+) \leq 0$. Then we have $Z(t_0) \leq m_0 - 1$.

We have to consider the last situation: $Z(t_0) = m_0 - 1$.

Let us assume that $Z(t_0) = m_0 - 1$, and that the trajectory goes into D_0. We can write

$$\begin{cases} \dot{X}(t_0^+) = 0 \quad \text{and} \quad \ddot{X}(t_0^+) = 0 \\ \dot{Y}(t_0) = 0 \\ \dot{Z}(t_0) = -\beta m_0 > 0 \end{cases} \tag{57}$$

Let us calculate $\dddot{X}(t_0^+)$. For $\eta > 0$ small enough we have

$$\dddot{X}(t_0+\eta) = \alpha(\ddot{Y}(t_0+\eta) - \ddot{X}(t_0+\eta)m_0)$$

and then

$$\begin{aligned} \dddot{X}(t_0+\eta) = \alpha(&\dot{X}(t_0+\eta) - \dot{Y}(t_0+\eta) \\ &+ \dot{Z}(t_0+\eta) - \alpha m_0(\dot{Y}(t_0+\eta) \\ &- m_0\dot{X}(t_0+\eta))) \end{aligned}$$

That yields

$$\begin{aligned} \dddot{X}(t_0^+) = \alpha[&(1+\alpha m_0^2)\dot{X}(t_0^+) \\ &- (1+\alpha m_0)\dot{Y}(t_0) + \dot{Z}(t_0)] \end{aligned}$$

that is $\dddot{X}(t_0^+) = -\alpha\beta m_0 > 0$. This situation cannot occur because $X(t_0+\eta) < 0$ has to be verified for every η small enough. Thus it is clear that the trajectory cannot go into D_0, which means that it stays in $X = 1$.

(b) If $Y(t_0) = m_0+\varepsilon$, the trajectory can either stay in $X = 1$ or reach D_1.

Let us look for a necessary condition for it to stay in $X = 1$: Some calculations lead to $Z(t_0) \leq m_0+\varepsilon-1$.

Let us look for a necessary condition for it to run into D_1: We find $Z(t_0) \geq m_0+\varepsilon-1$.

Then we have to study the last case $Z(t_0) = m_0+\varepsilon-1$.

If $Z(t_0) = m_0+\varepsilon-1$ one has

$$\begin{cases} \dot{X}(t_0^+) = 0 \\ \dot{Y}(t_0^+) = 0 \\ \dot{Z}(t_0) = -\beta(m_0+\varepsilon) > 0 \end{cases}$$

and

$$\ddot{Y}(t_0) = \dot{X}(t_0^+) - \dot{Y}(t_0) + \dot{Z}(t_0) = -\beta(m_0+\varepsilon) > 0$$

Hence $\dot{Y}$ is strictly increasing after t_0, and then $Y(t_0+\eta) > Y(t_0) = m_0+\varepsilon$ for η small enough and the trajectory goes into D_1.

We can sum up the different behaviors of the trajectory at the crossing of $X = 1$:

— The trajectory goes into D_1 if $Y(t_0) > m_0+\varepsilon$ or $(Y(t_0) = m_0+\varepsilon$ and $Z(t_0) \geq m_0+\varepsilon-1)$

— The trajectory goes into D_0 if $Y(t_0) < m_0$ or $(Y(t_0) = m_0$ and $Z(t_0) < m_0-1)$

— the trajectory stays in $X = 1$ if $m_0 < Y(t_0) < m_0+\varepsilon$ or $(Y(t_0) = m_0+\varepsilon$ and $Z(t_0) < m_0+\varepsilon-1)$ or $(Y(t_0) = m_0$ and $Z(t_0) \geq m_0-1)$.

Let us notice that we have only established necessary conditions: The same calculations provide the sufficient conditions.

5.1.2. *Case 2: Discontinuity at* 0

In this second example it is sufficient to determine the crossing at $X = 0$. Let us introduce $D_0^- =]-1, 0[\times\mathbb{R}^2$ and $D_0^+ =]0, 1[\times\mathbb{R}^2$. Starting from a given t_0 so that $X(t_0) = 0$, it is possible to study three cases (the trajectory goes into D_0^- or D_0^+, or it stays in $X = 0$). Calculations are similar to the previous example. The results can be summed up as follows:

— The trajectory runs into D_0^+ if $Y(t_0) > \varepsilon$ or $(Y(t_0) = \varepsilon$ and $Z(t_0) > \varepsilon)$
— The trajectory runs into D_0^- if $Y(t_0) < -\varepsilon$ or $(Y(t_0) = -\varepsilon$ and $Z(t_0) < -\varepsilon)$
— The trajectory stays in $X = 0$ if $-\varepsilon < Y(t_0) < \varepsilon$ or $(Y(t_0) = \varepsilon$ and $Z(t_0) \le \varepsilon)$ or $(Y(t_0) = -\varepsilon$ and $Z(t_0) \ge -\varepsilon)$

5.2. *Analytical calculation of the solution*

5.2.1. *Discontinuity at* -1 *and* 1

We define u_1, C_1, C_0, $\mathcal{L}_1$ and T_1 according to Appendix 1. We assume that the numerical values of the parameters provide one real eigenvalue and two complex conjugate ones [Kuznetsov *et al.*, 1996] (this is verified by every parameter that will be used for numerical examples).

We have to solve the following problem:

$$\begin{cases} \dot{y} = C_1 y + u_1 & \text{on } D_1 =]1, +\infty[\times\mathbb{R}^2 \\ \dot{y} = C_0 y & \text{on } D_0 =]-1, 1[\times\mathbb{R}^2 \\ \dot{y} = C_1 y - u_1 & \text{on } D_{-1} =]-\infty, -1[\times\mathbb{R}^2 \end{cases} \tag{58}$$

Each equation is a linear one: It is easy to find the solution whatever the initial condition. The key point is to find successive times when the coordinate $X(t)$ crosses a plane of discontinuity $X = -1$ or $X = 1$. This is done by solving scalar nonlinear equations depending on t and by using the results of Sec. 5.1.1.

5.2.2. *Discontinuity at* 0

We introduce C_0', u_1', $\mathcal{L}_0$ and T_0 according to Appendix 2. We assume that the numerical values of the parameters provide one real eigenvalue and two complex conjugates ones [Kuznetsov *et al.*, 1996] (this is again verified by every parameter that will be used for numerical examples).

We have to solve the following problem:

$$\begin{cases} \dot{y} = C_1 y + u_1' & \text{on } D_1 =]1, +\infty[\times\mathbb{R}^2 \\ \dot{y} = C_0' y + u_0 & \text{on } D_0^+ =]0, 1[\times\mathbb{R}^2 \\ \dot{y} = C_0' y - u_0 & \text{on } D_0^- =]-1, 0[\times\mathbb{R}^2 \\ \dot{y} = C_1 y - u_1' & \text{on } D_{-1} =]-\infty, -1[\times\mathbb{R}^2 \end{cases} \tag{59}$$

Again each linear equation can be solved. Scalar nonlinear equations depending on t have to be solved to determine the crossing of $X = 0$. Results of Sec. 5.1.2 are used to calculate the solution after the meeting of discontinuity.

6. Numerical Results

6.1. *First example: Discontinuities at* -1 *and* 1

6.1.1. *Bifurcation diagram*

In order to test the occurrence of chaos, we study bifurcation diagrams. In Fig. 3, such a bifurcation diagram is presented for the following parameter values:

$$m_0 = -\frac{1}{7} \quad m_1 = \frac{2}{7} \quad \alpha = 3.612 \quad \beta = 4.4$$

and ε varies from 0. to 1/7. In this diagram

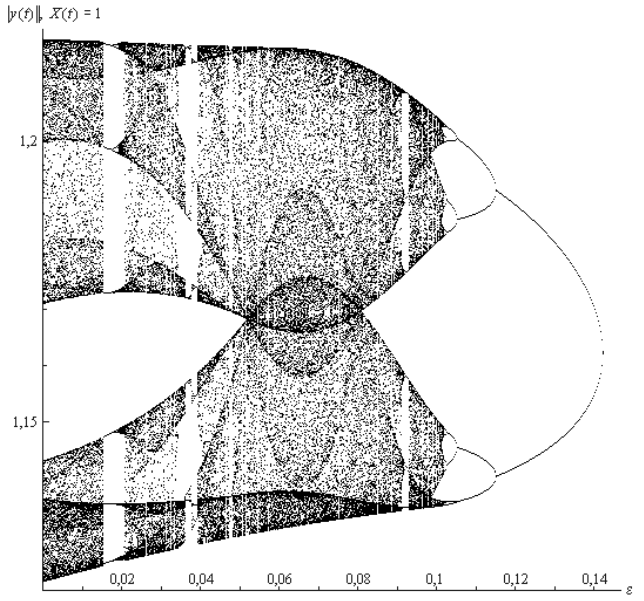

Fig. 3. Bifurcation diagram for $\alpha = 3.612$ and $\beta = 4.4$ for the system with discontinuities at -1 and 1.

Table 1. Analysis of the bifurcation cascade.

Period	Parameter, ε_k	Ratio, δ_{k-2}
1	$\varepsilon_0 = 0.1425252608 \pm 10^{-10}$	
2	$\varepsilon_1 = 0.115436145850 \pm 10^{-12}$	
4	$\varepsilon_2 = 0.105493669499 \pm 10^{-12}$	$\delta_0 = 2.725$
8	$\varepsilon_3 = 0.102879706220 \pm 10^{-12}$	$\delta_1 = 3.804$
16	$\varepsilon_4 = 0.102286178168 \pm 10^{-12}$	$\delta_2 = 4.404$
32	$\varepsilon_5 = 0.102155640398 \pm 10^{-12}$	$\delta_3 = 4.547$
64	$\varepsilon_6 = 0.102126753995 \pm 10^{-12}$	$\delta_4 = 4.519$
128	$\varepsilon_7 = 0.102120342667 \pm 10^{-12}$	$\delta_5 = 4.506$
256	$\varepsilon_8 = 0.10211894039545 \pm 10^{-14}$	$\delta_6 = 4.572$
512	$\varepsilon_9 = 0.10211858239154 \pm 10^{-14}$	$\delta_5 = 3.917$
1024	$\varepsilon_{10} = 0.1021185049383287 \pm 10^{-16}$	$\delta_5 = 4.622$

we do not plot transient i.e. we plot $\|y(t)\| = \sqrt{X(t)^2 + Y(t)^2 + Z(t)^2}$ such as $X(t) = 1$ for $3000 \leq t \leq 4000$. Obviously chaos seems to occur and after some chaotic and periodic windows, chaos disappears via a cascade.

6.1.2. *Analysis of the cascade*

Here we test numerically the first terms of the series (introduced by Feigenbaum [1978]) $\delta_{k-1} = (\varepsilon_k - \varepsilon_{k-1})/(\varepsilon_{k+1} - \varepsilon_k)$ with ε_{k-1} the value of ε such as a bifurcation from a 2^{k-1} cycle to a 2^k one. The results are presented in Table 1. Periodic solutions are searched for $t \geq 50\,000$.

It seems that these results are slowly converging to the universal value $4.66920\ldots$.

6.2. *Second example: Discontinuities at* 0

6.2.1. *Bifurcation diagram*

This section is devoted to the bifurcation diagrams obtained for different values of the pair (α, β). In Fig. 4, such a bifurcation diagram is presented for $\alpha = 3.612$, $\beta = 4.4$ with ε varying from 0. to 0.025. Again $\|y(t)\|$ is plotted versus ε for $3000 \leq t \leq 4000$ when $X(t) = 1$. In this diagram several attractors seem to coexist: In the first two periodic windows, bifurcation branches show jumps. Just before ε reaches the value 0.025 the point (0., 0., 0.) captures the solutions. Indeed the trajectory issued from the initial conditions $(X_0, Y_0, Z_0) = (1.4, -0.3, -1.)$ is trapped by (0., 0., 0.) for $t \geq 100\,000$ if $\varepsilon \geq 0.024882$.

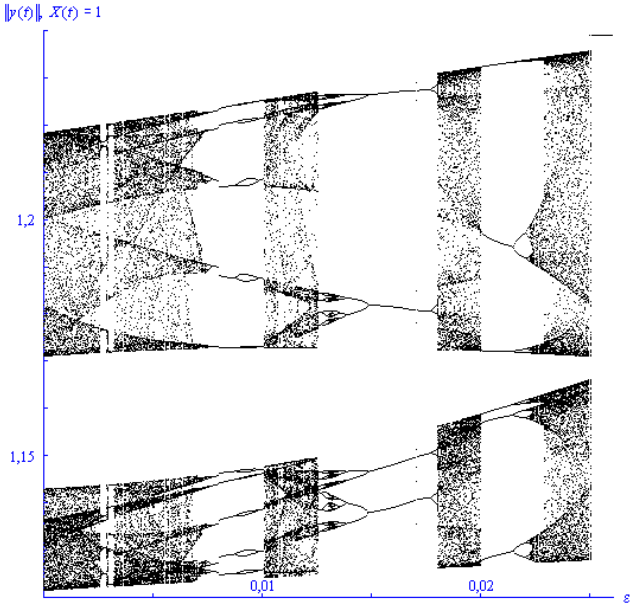

Fig. 4. Bifurcation diagram for $\alpha = 3.612$ and $\beta = 4.4$ for the system with discontinuity at 0.

Such a coexistence is clearer if we choose $\alpha = 15.6$, $\beta = 28.58$. In Figs. 5(a) and 5(b) where ε varies from 0. to 0.055, we can see two parts of the same diagram: Chaos and periodic solutions coexist for $\varepsilon = 0.0005$ and $\varepsilon = 0.009$ for example. Phase portraits are showed in the next subsection in order to clarify this point.

6.2.2. *Phase portraits*

Let us consider the first case ($\alpha = 3.612$, $\beta = 4.4$): Several phase portraits are presented in Figs. 6(a)–6(l) for $\varepsilon = 0.$, $\varepsilon = 0.0027$, $\varepsilon = 0.005$, $\varepsilon = 0.008$, $\varepsilon = 0.0103$, $\varepsilon = 0.016$, $\varepsilon = 0.018$, $\varepsilon = 0.0205$, $\varepsilon = 0.0227$, $\varepsilon = 0.02488$, $\varepsilon = 0.02489$, $Y(t)$ is plotted versus $X(t)$ except for Fig. 6(l) $\varepsilon = 0.02489$ where $Y(t)$ is plotted versus $Z(t)$. Both chaotic and periodic solutions are obtained. For the last two graphics of this figure, we can see that after a rather long and chaotic-like transient ($t = 41\,969$) the solution is trapped to $(0., 0., 0.)$. It means that when exerting a friction-like action on the Chua oscillator we obtain a passive control of nonlinear oscillations. We shall investigate the area of control in phase space in another section.

Now let us consider the second case associated with $\alpha = 15.6$, $\beta = 28.58$. In Figs. 7(a) and 7(b) phase portraits of the two different attractors obtained for $\varepsilon = 0.005$ are plotted: $Y(t)$ is plotted versus $X(t)$. One is chaotic and the other one is periodic. The same kind of behavior is obtained for

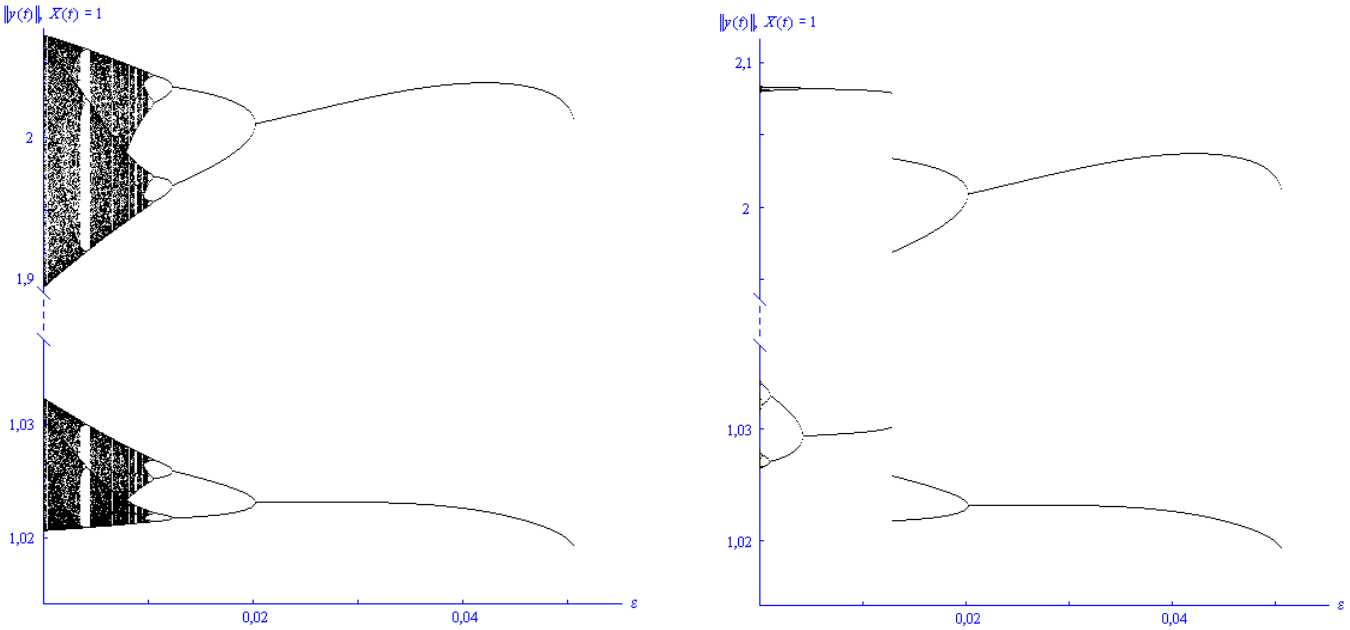

(a) (b)

Fig. 5. Bifurcation diagrams (a) and (b) for $\alpha = 15.6$ and $\beta = 28.58$ for the system with discontinuity at 0.

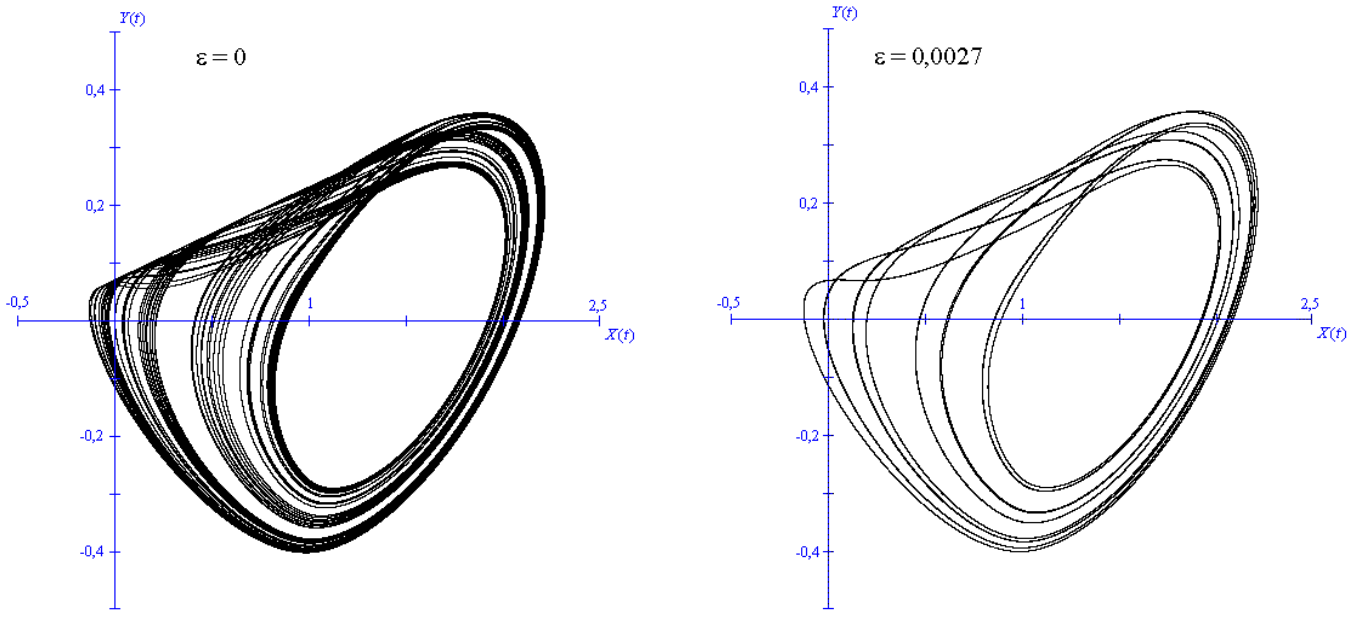

(a) (b)

Fig. 6. (X, Y)-phase portrait for $\alpha = 3.612$, $\beta = 4.4$ and (a) $\varepsilon = 0.$, (b) $\varepsilon = 0.0027$, (c) $\varepsilon = 0.005$, (d) $\varepsilon = 0.008$, (e) $\varepsilon = 0.0103$, (f) $\varepsilon = 0.016$, (g) $\varepsilon = 0.018$, (h) $\varepsilon = 0.0205$, (i) $\varepsilon = 0.0227$, (j) $\varepsilon = 0.02488$, (k) $\varepsilon = 0.02489$, (Y, Z)-phase portrait for $\alpha = 3.612$, $\beta = 4.4$ and (l) $\varepsilon = 0.02489$.

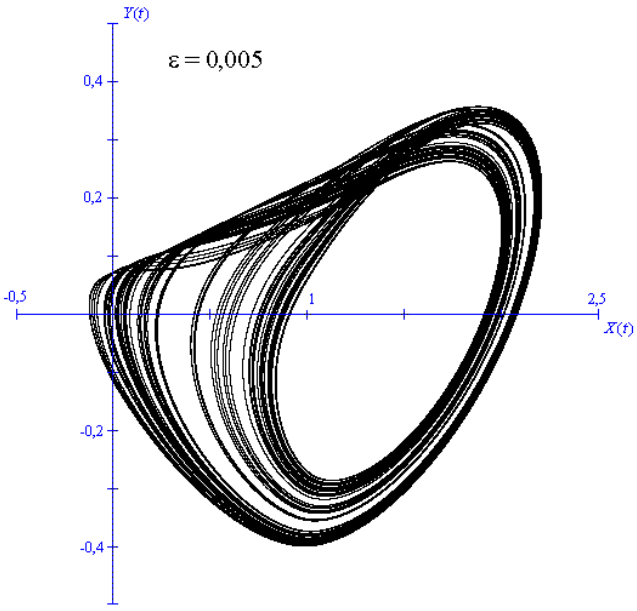

(c)

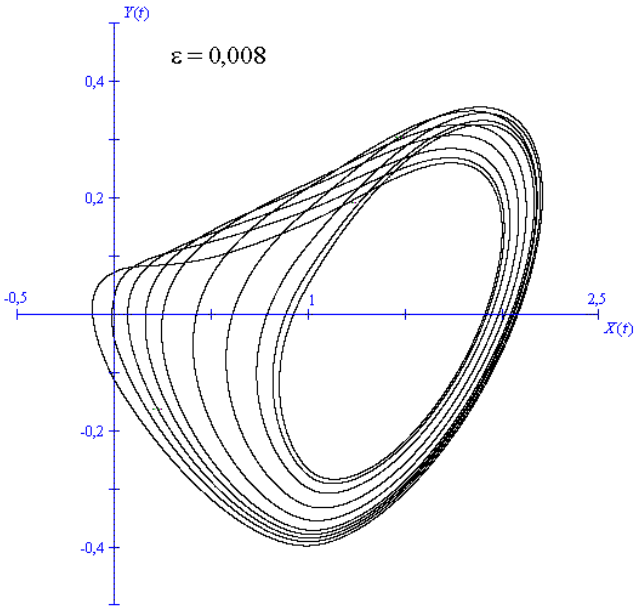

(d)

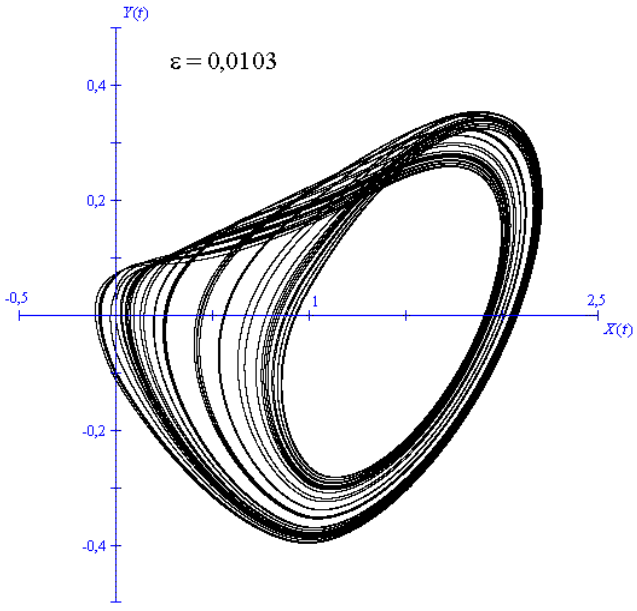

(e)

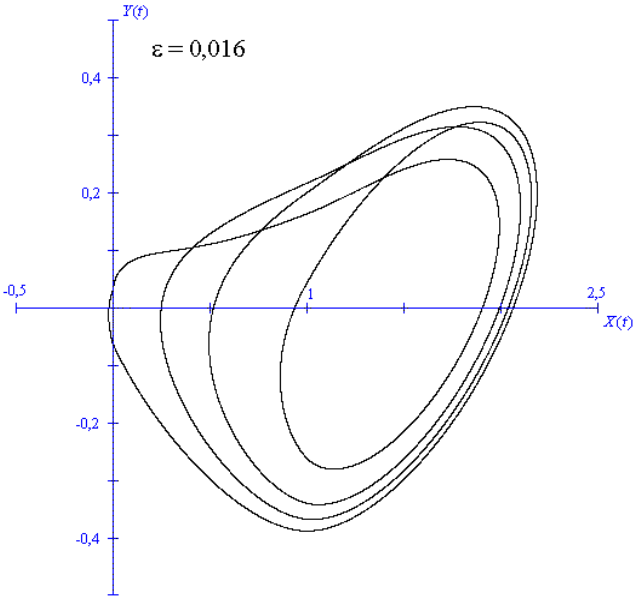

(f)

Fig. 6. (*Continued*)

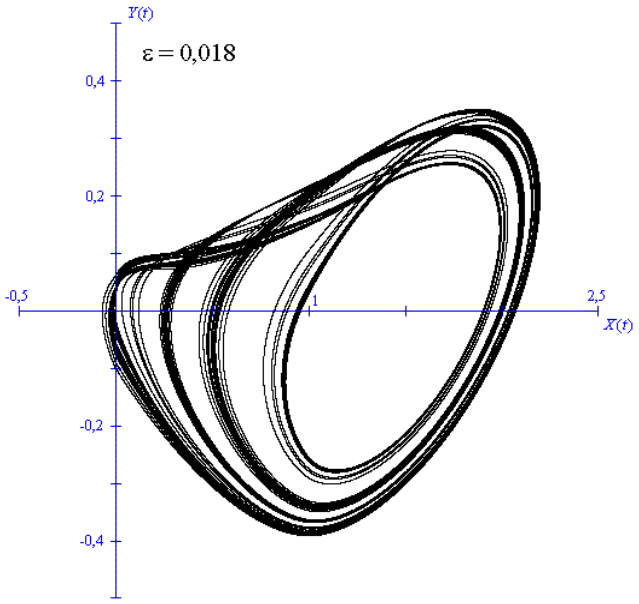

(g)

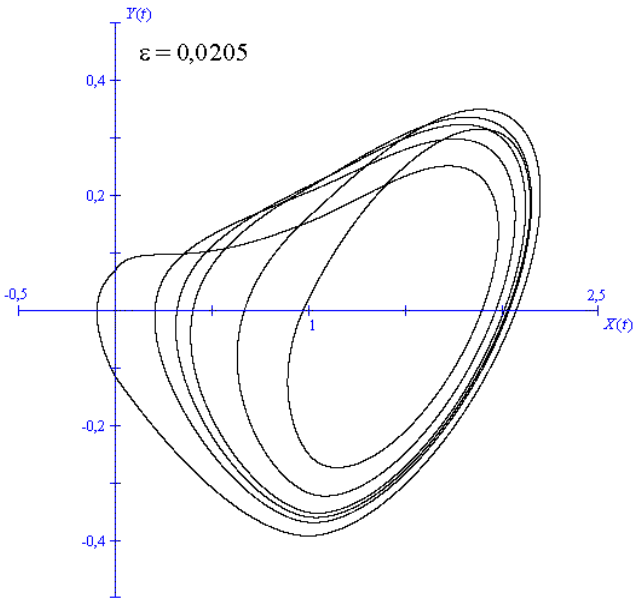

(h)

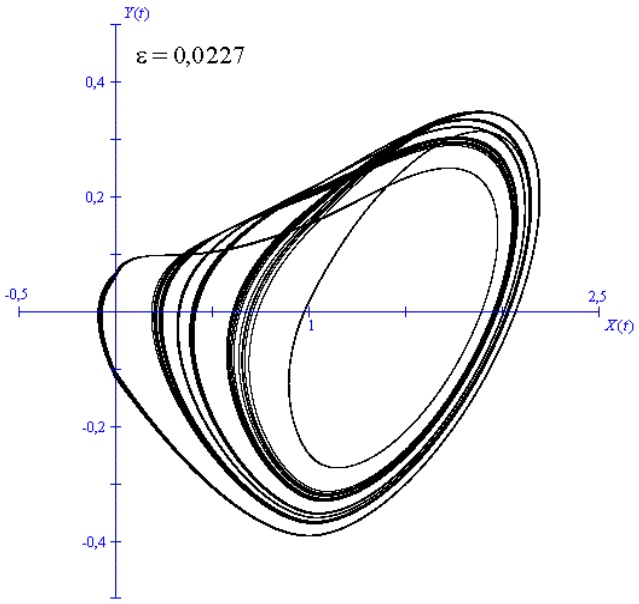

(i)

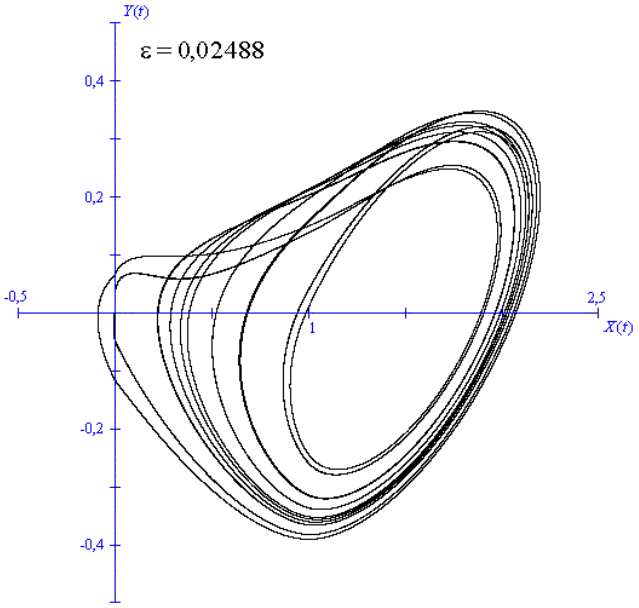

(j)

Fig. 6. (*Continued*)

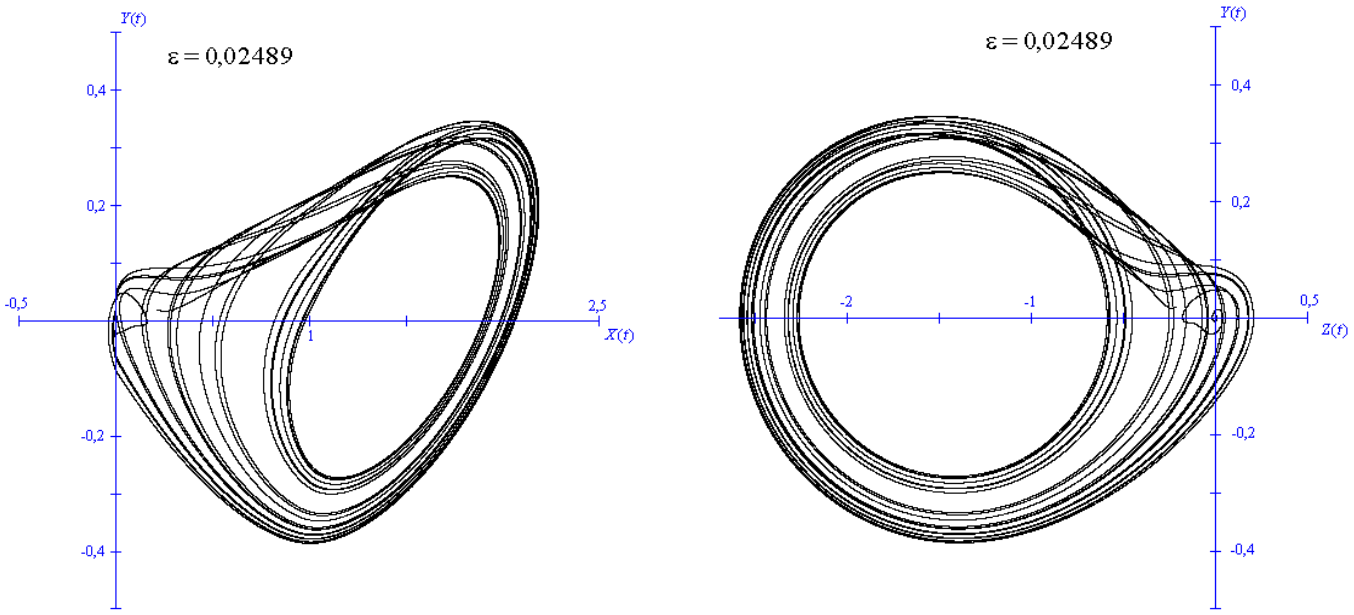

(k) (l)

Fig. 6. (*Continued*)

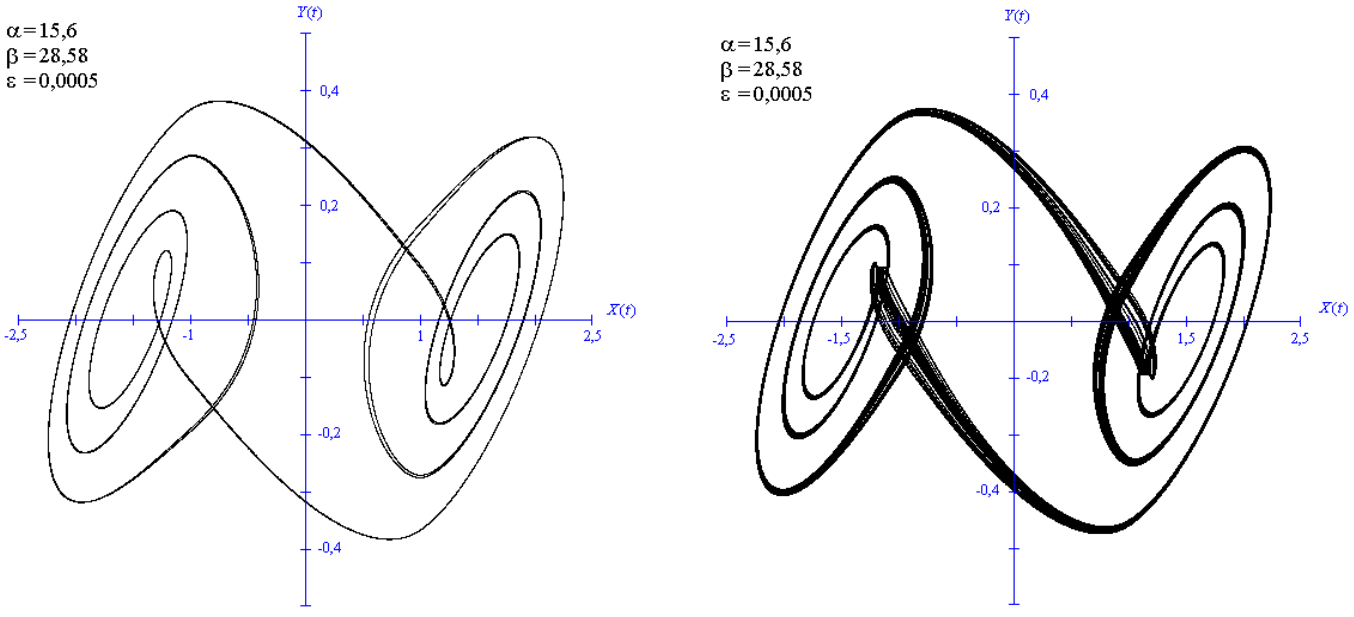

(a) (b)

Fig. 7. (X, Y)-phase portrait for $\alpha = 15.6$, $\beta = 28.58$ and $\varepsilon = 0.0005$, with initial conditions (a) $X_0 = 1$, $Y_0 = 0.096$, $Z_0 = -1.815$ and (b) $X_0 = 1.4$, $Y_0 = -0.3$, $Z_0 = -1$ for the system with discontinuity at 0.

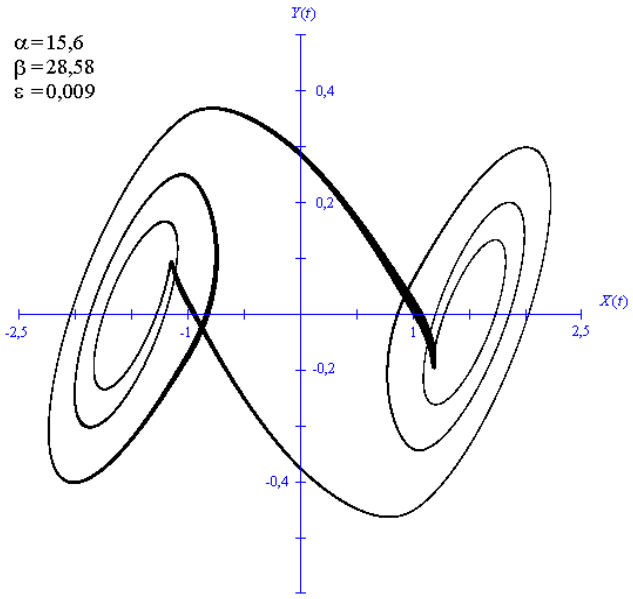

(a)

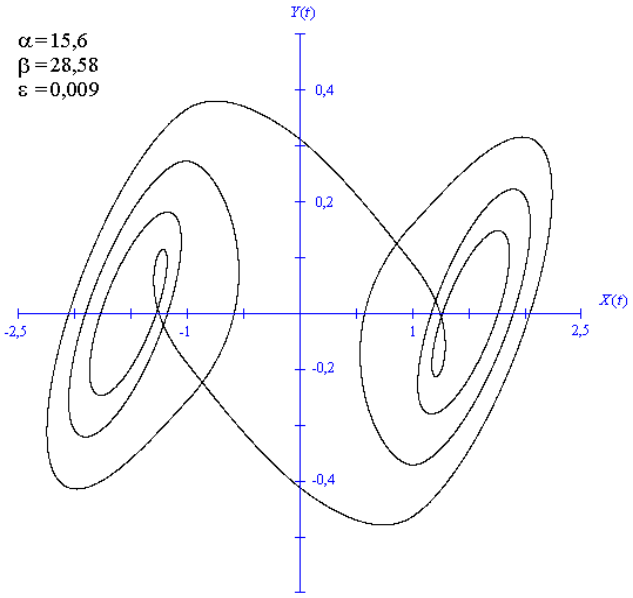

(b)

Fig. 8. (X, Y)-phase portrait for $\alpha = 15.6$, $\beta = 28.58$ and $\varepsilon = 0.0009$, with initial conditions (a) $X_0 = 1$, $Y_0 = 0$, $Z_0 = -1.74$ and (b) $X_0 = 1.4$, $Y_0 = -0.3$, $Z_0 = -1$ for the system with discontinuity at 0.

$\varepsilon = 0.009$: In Fig. 8 one can see one periodic attractor and one chaotic attractor. In these two cases the periodic and the chaotic attractor are quite "close" to each other in phase space.

6.2.3. *Poincaré maps and trapping area*

Here we deal with Poincaré maps corresponding to $(\alpha = 3.612,\ \beta = 4.4)$ and $\varepsilon = 0.$, $\varepsilon = 0.0027$, $\varepsilon = 0.005$, $\varepsilon = 0.008$, $\varepsilon = 0.0103$, $\varepsilon = 0.016$, $\varepsilon = 0.018$, $\varepsilon = 0.0205$, $\varepsilon = 0.0227$, $\varepsilon = 0.02488$, $\varepsilon = 0.02489$ as in the previous subsection. In Fig. 9 such sections are plotted in the plane $X = 0$ together with the trapping area of (0., 0., 0.). This yellow area has been calculated numerically. Any trajectory crossing through this area will not be able to escape and will converge to the equilibrium point (0., 0., 0.).

We can see that the trapping phenomenon is not related to the intersection between the trapping area and the "transient attractor". It seems that friction provides the beginning of intermittent behavior that is suppressed by the trapping: Once a trajectory enters the trapping area it can never go out anymore.

6.2.4. *Trapping solutions and basins of attraction*

We have seen previously that for values of ε large enough, the trajectories starting from some initial conditions are trapped to $(0., 0., 0.)$. In order to determine whether that is the case for every initial condition, we have used a cell-mapping method [Hsu, 1987] to compute the set of initial conditions included into $X = 0$ that lead to a trapping phenomenon. This method consists in defining a grid in $\{0\} \times [-2, 2] \times [-2, 2]$. Then for each cell on this grid we take the center as an initial condition, calculate the flow and determines where it hits on the plane $X = 0$ again. That gives a map from $\{0\} \times [-2, 2] \times [-2, 2]$ to $\{0\} \times \mathbb{R}^2$. This map is iterated (and restrained to $\{0\} \times [-2, 2] \times [-2, 2]$ at every iteration) 1000 times. Results for $\varepsilon = 0.02$ and $\varepsilon = 0.04$ are shown in Figs. 10(a) and 10(b). The black area corresponds to trapped solutions and the white area stands for divergent solutions. The two colours (blue and red) distinguish the solutions that start from $X = 0$ and then go to the domain D_0^+ from solutions that start from $X = 0$ and then go to the domain D_0^-.

It can be seen that before ($\varepsilon = 0.02$) the critical parameter $\varepsilon \simeq 0.02488$, the trapping area is small and concentrated in the neighborhood of (0., 0., 0.). After ($\varepsilon = 0.04$) the critical parameter, the whole nondivergent area is caught by $(0., 0., 0.)$ (for the same time interval): It means that every trajectory starting from any initial condition in $\mathbb{R}^3$ will either be trapped to $(0., 0., 0.)$ or diverge to infinity.

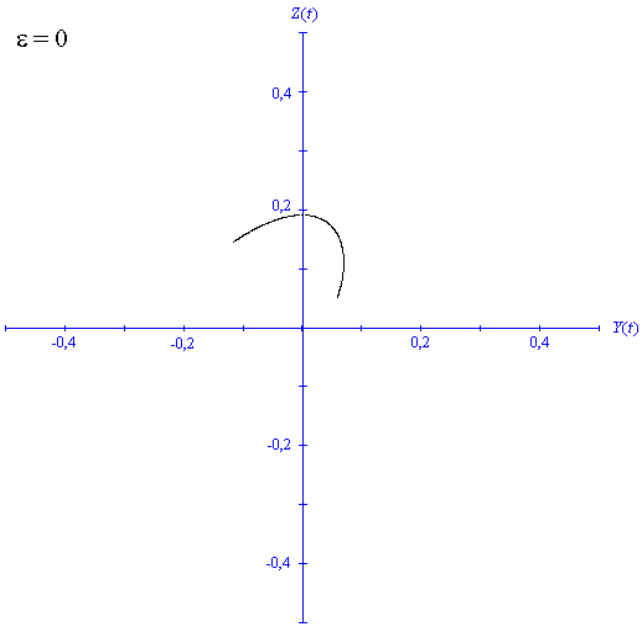

(a)

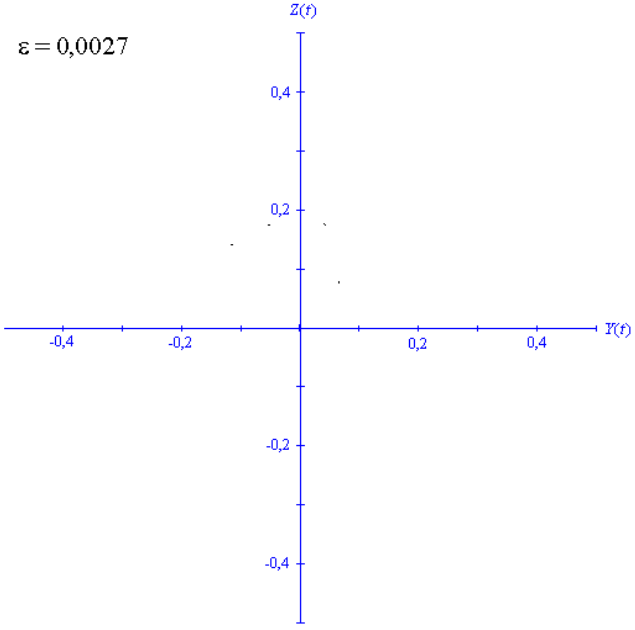

(b)

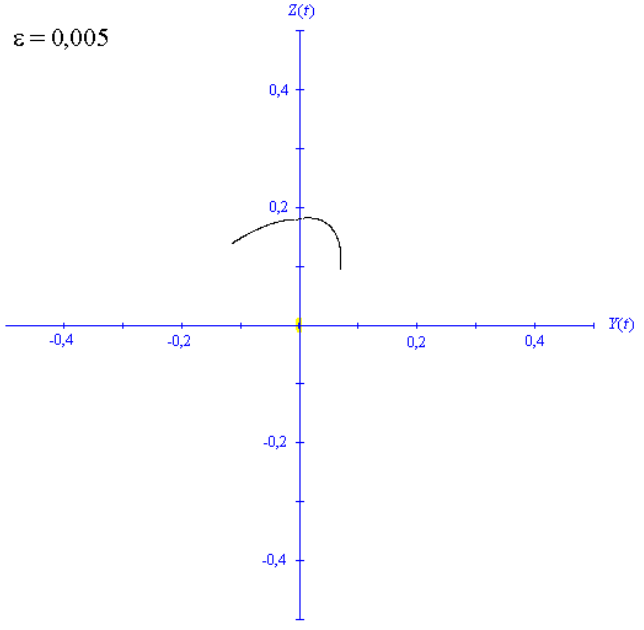

(c)

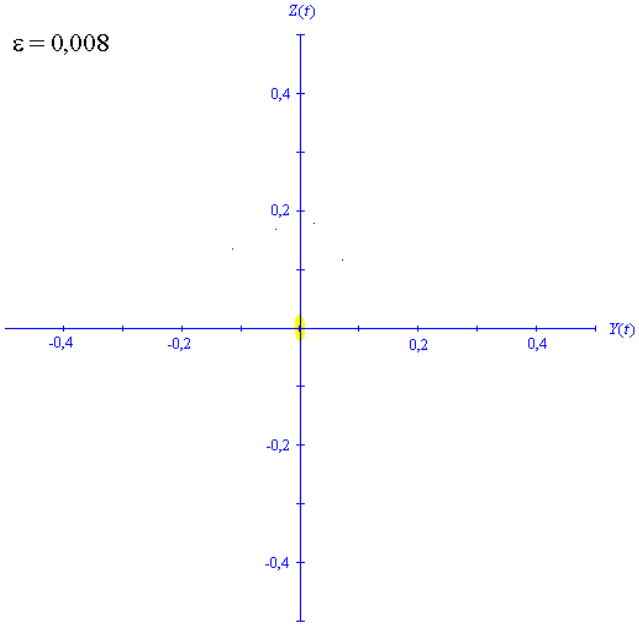

(d)

Fig. 9. Poincaré section in the plane $X = 0$ with trapping area, for $\alpha = 3.612$, $\beta = 4.4$ and (a) $\varepsilon = 0$, (b) $\varepsilon = 0.0027$, (c) $\varepsilon = 0.005$, (d) $\varepsilon = 0.008$, (e) $\varepsilon = 0.0103$, (f) $\varepsilon = 0.016$, (g) $\varepsilon = 0.018$, (h) $\varepsilon = 0.0205$, (i) $\varepsilon = 0.0227$, (j) $\varepsilon = 0.02488$, (k) $\varepsilon = 0.02489$ for the system with discontinuity at 0.

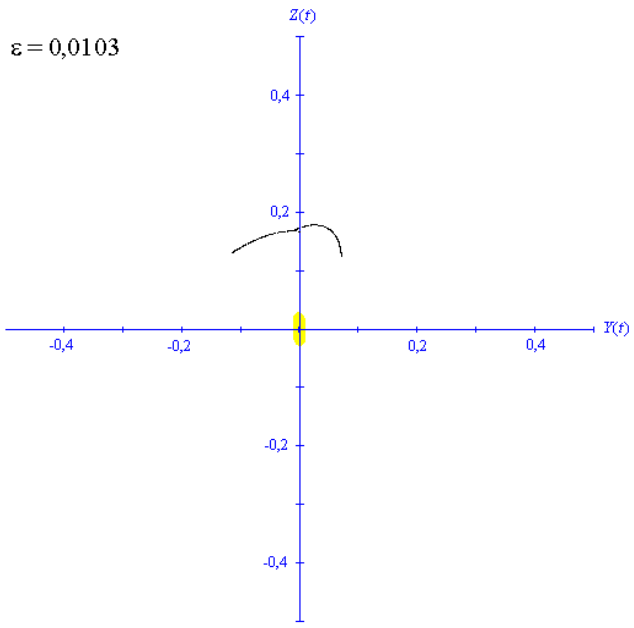

(e)

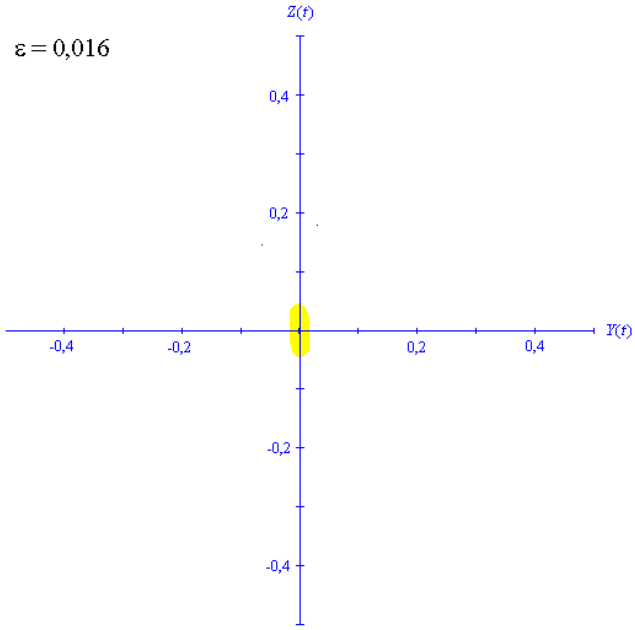

(f)

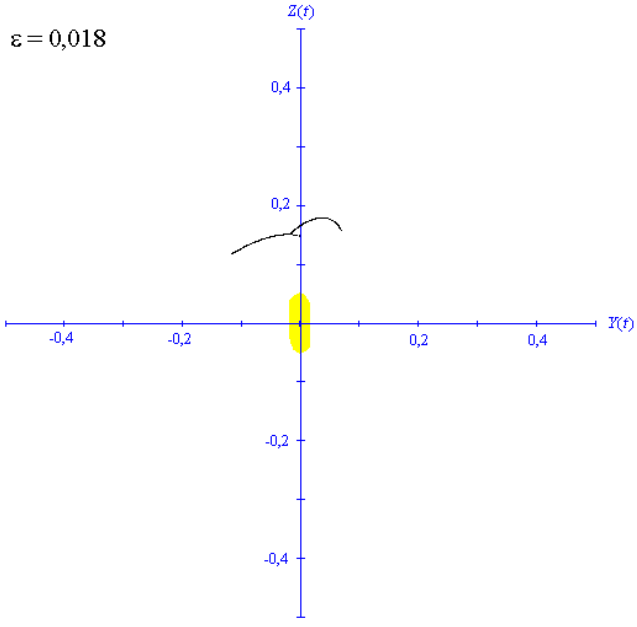

(g)

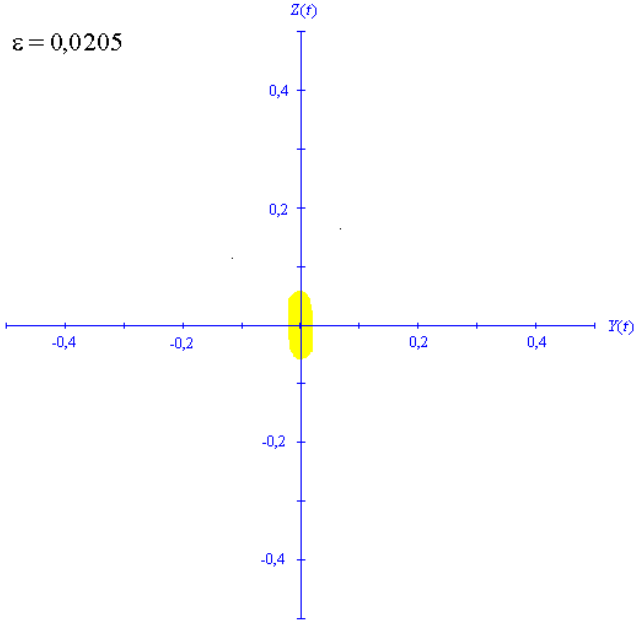

(h)

Fig. 9. (*Continued*)

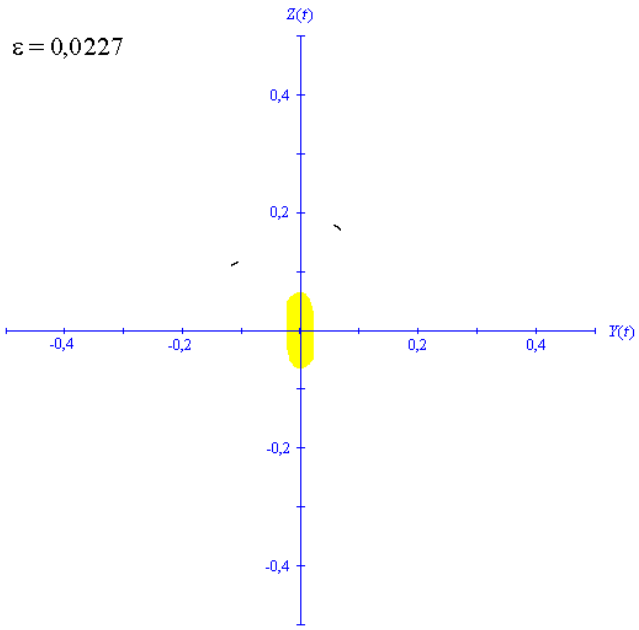

(i)

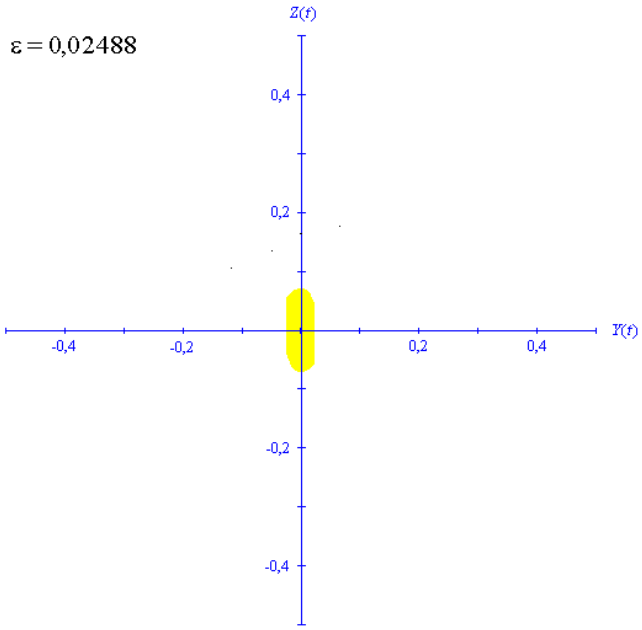

(j)

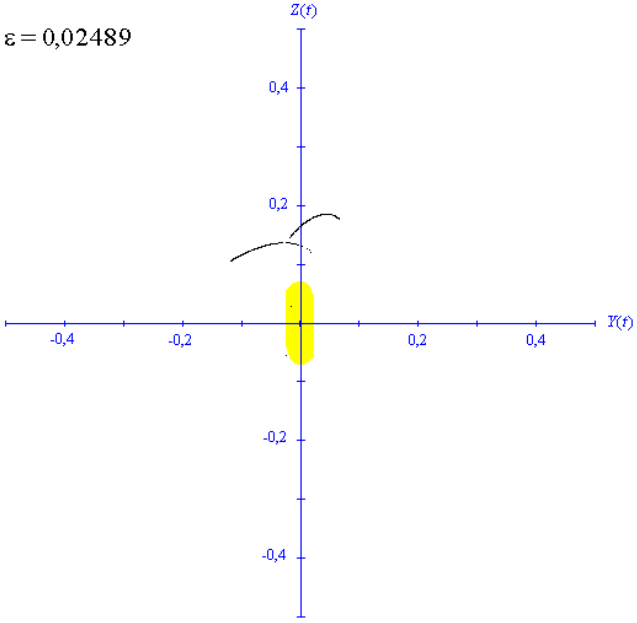

(k)

Fig. 9. (*Continued*)

6.2.5. *Lyapunov exponents*

6.2.5.1. Methods

In the special case of piecewise-linear differential systems, four methods at least could be used to compute Lyapunov exponents.

The first one consists in estimating analytically the value $D\varphi/DX_0$ for on each area where the system is linear, the flow φ can be expressed analytically as a function of the initial condition. With the second method, the flow is still calculated analytically but the differentiation is this time a

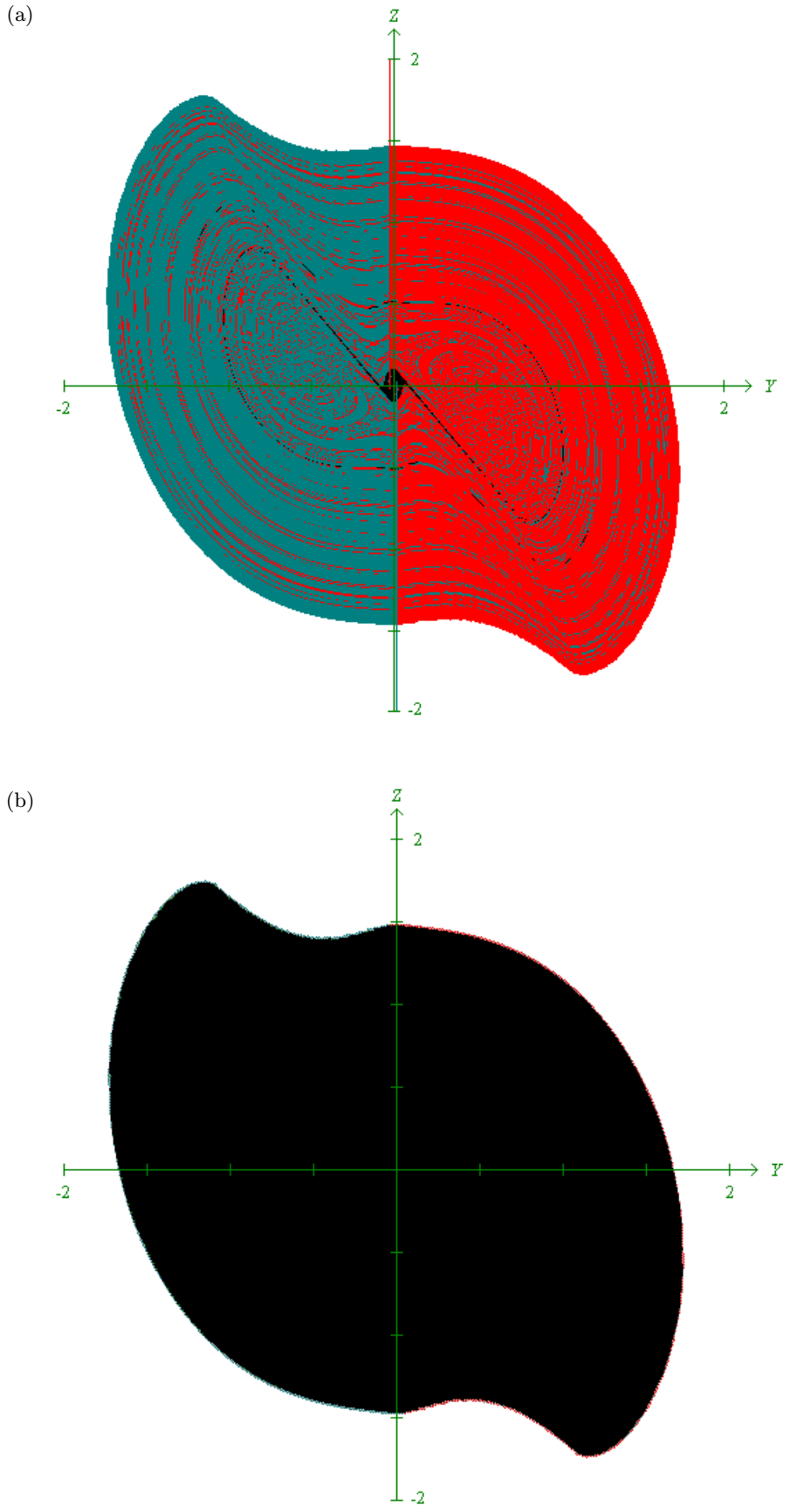

Fig. 10. Trapping area in the plane $X = 0$ for $\alpha = 3.612$, $\beta = 4.4$ and (a) $\varepsilon = 0.02$, (b) $\varepsilon = 0.04$.

Table 2. Largest Lyapunov exponent for $\alpha = 3.612$ and $\beta = 4.4$ after $T = 100\,000$.

Epsilon	$\lambda_{\max}$
0	0.04777
0.0027	0.00027
0.005	0.03800
0.008	0.00005
0.0103	0.03970
0.016	0.00002
0.018	0.02792
0.0205	0.00008
0.0227	0.01507
0.02488	0.03226

numerical one. A third method uses numerical schemes to build the flow, but then it requires an analytical differentiation of the estimated flow. The last method is fully numerical: Both the trajectory and the differential $D\varphi/DX_0$ are estimated by numerical devices.

The method that we have chosen here is the second one. Indeed, the first method is very time expensive, and the last two were not used because they do not benefit from the piecewise linearity of the system, which allows analytical calculation of the trajectories.

The method used consists in starting with two very close initial conditions and building analytically their trajectories. At regular intervals, the trajectories are rescaled and a computation of $D\varphi/DX_0$ is performed. This method provides an estimation of the biggest Lyapunov exponent of the dynamical system, which is enough to check the presence of chaos.

6.2.5.2. Results

The largest Lyapunov exponent $\lambda_{\max}$ was computed for several parameter values which have already been used in Secs. 6.2.2 and 6.2.3. Table 2 shows the results corresponding to Figs. 6(a)–6(j): We can see a good correlation between phase portrait and Lyapunov exponents, except for the case $\varepsilon = 0.02488$ where phase portrait and Poincaré section suggest that there is a periodic attractor, whereas $\lambda_{\max}$ seems to be clearly positive [see Fig. 11(c)].

In Figs. 11(a)–11(c) we have plotted the value of $\lambda_{\max}$ as a function of time to check the stabilization of calculations. It appears that at $t = 100\,000$, $\lambda_{\max}$ has only small variations so that we can give its final value with a 10^{-3} uncertainty at most.

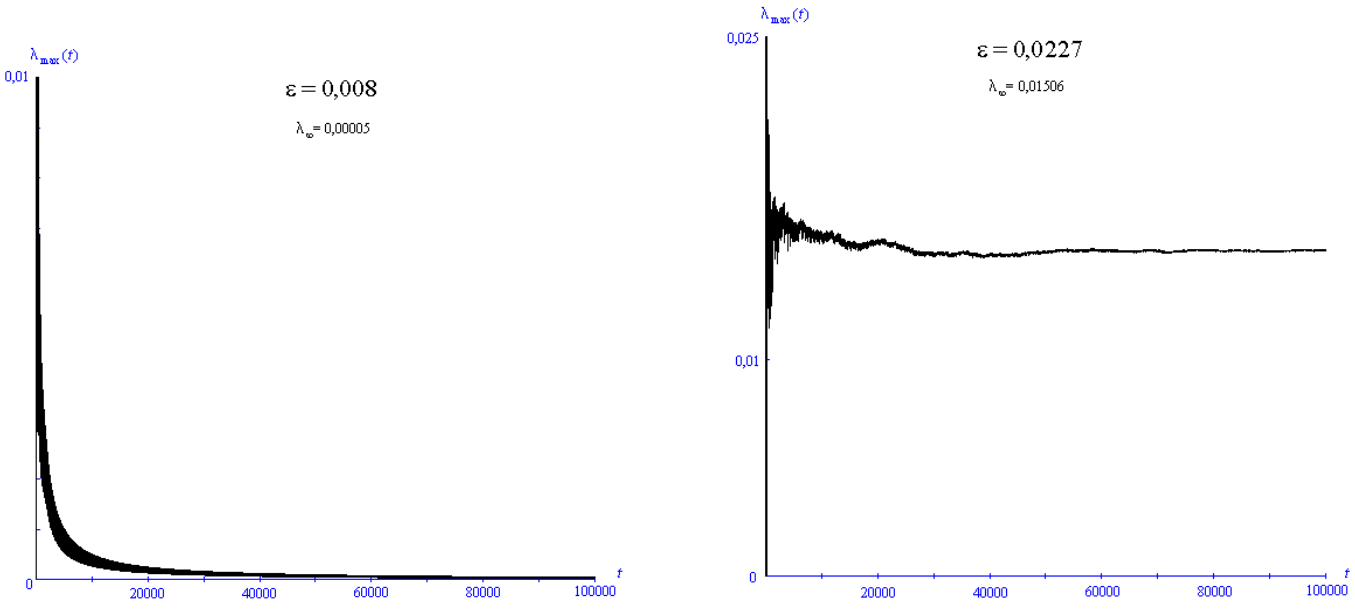

(a) (b)

Fig. 11. Evolution of the largest Lyapunov exponent versus time for $\alpha = 3.612$, $\beta = 4.4$ and (a) $\varepsilon = 0.008$, (b) $\varepsilon = 0.0227$, (c) $\varepsilon = 0.02488$ for the system with discontinuity at 0.

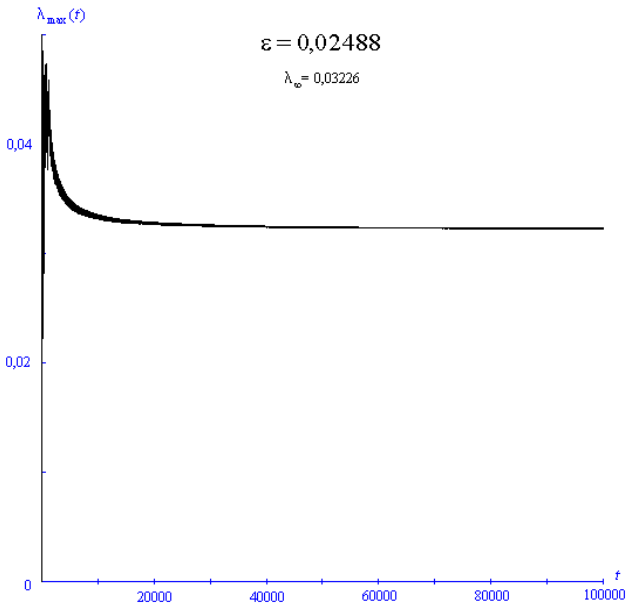

(c)

Fig. 11. (*Continued*)

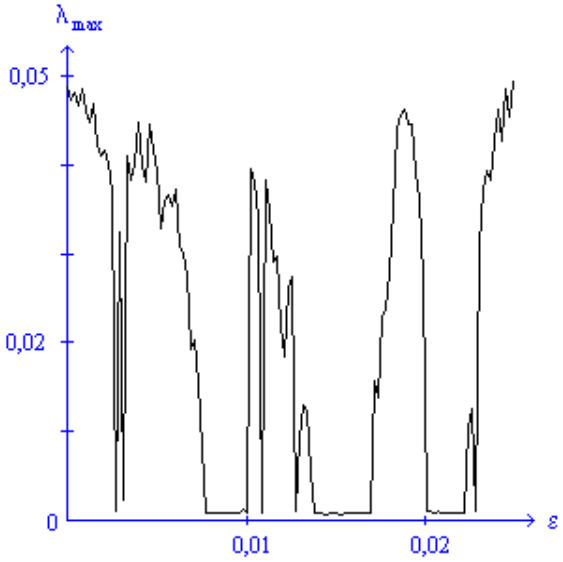

Fig. 12. Evolution of the largest Lyapunov exponent versus ε for $\alpha = 3.612$, $\beta = 4.4$ and for the system with discontinuity at 0.

Finally, in Fig. 12 the value of $\lambda_{\max}$ for $t = 40\,000$ was plotted as a function of ε, with the same parameter values as in Fig. 4. Both figures show good correlation, every periodic window corresponding to values $\lambda_{\max} \leq 0.001$ and every chaotic one to values more clearly positive.

Finally, we present the computation of Lyapunov exponents split into four parts: The calculation is made up to $T = 100\,000$, and every time the trajectory enters a domain (D_1, D_{0^+}, D_{0^-} or D_{-1}) we keep the time spent in that domain and the contribution to the calculation of the largest Lyapunov exponent. Thus we define λ_1, λ_{0^+}, λ_{0^-} or λ_{-1} as follows:

$$\lambda_i = \frac{1}{\sum\limits_n t_n^i} \ln \left(\prod_n \frac{\Delta y_n^i}{\Delta y_{n-1}^i} \right) \tag{60}$$

where t_n is the nth time spent in domain D_i, $\Delta y_n^i / \Delta y_{n-1}^i$ the corresponding contribution to $\lambda_{\max}$, and $i \subset \{1, 0^+, 0^-, -1\}$. Results are shown in Table 3, together with every $T_i = \sum_n t_n^i$, for $\alpha = 15.6$, $\beta = 28.58$ and $\varepsilon = 0$ with two different initial conditions. It appears that these partial exponents are good indicators of the symmetry of attractors which is not obvious at first sight: For symmetric ones, we have $\lambda_1 = \lambda_{-1}$ and $\lambda_{0^+} = \lambda_{0^-}$, whereas for nonsymmetric ones, all λ_i are different. Moreover, an averaging formula holds for the calculation of the largest Lyapunov exponent: one has

$$\lambda_{\max} = \frac{T_1\lambda_1 + T_{0^+}\lambda_{0^+} + T_{0^-}\lambda_{0^-} + T_{-1}\lambda_{-1}}{T_1 + T_{0^+} + T_{0^-} + T_{-1}} \tag{61}$$

Table 3. Partial Lyapunov exponents for $\alpha = 15.6$, $\beta = 28.58$ and $\varepsilon = 0$. (a) $X_0 = -0.002$, $Y_0 = 0.014$, $Z_0 = 0.010$, (b) $X_0 = -0.008$, $Y_0 = 0.020$, $Z_0 = 0.028$.

	Exponent	Time
(a)	$\lambda_1 = -0.09435$	$T_1 = 40181$
	$\lambda_{0^+} = -0.04497$	$T_{0^+} = 9591$
	$\lambda_{0^-} = -0.21074$	$T_{0^-} = 10179$
	$\lambda_{-1} = 0.22839$	$T_{-1} = 40053$
	$\lambda_{\max} = 0.02780$	$T = 100004$
(b)	$\lambda_1 = 0.38000$	$T_1 = 39644$
	$\lambda_{0^+} = -1.01647$	$T_{0^+} = 9169$
	$\lambda_{0^-} = -1.00361$	$T_{0^-} = 9161$
	$\lambda_{-1} = 0.37334$	$T_{-1} = 39657$
	$\lambda_{\max} = 0.11632$	$T = 97631$

7. Conclusion

In this paper, we have investigated a mechanical model which can be written as a Chua circuit

with discontinuities. Existence and uniqueness have been obtained in the frame of monotonous maximal operators. Then analytical procedures have been developed in order to track the discontinuity times. Thus numerical results are provided including the detection of discontinuity with a very high accuracy. Discontinuities seem to provide symmetry breaking. Chaos has been observed. It has been characterized by positive Lyapunov exponent.

Discontinuities may correspond to a kind of friction from the mechanical point of view. We have shown that it is possible to control the Chua circuit: If the discontinuity is strong enough, every initial condition starting from a neighborhood of $(0, 0, 0)$ is trapped to this equilibrium point.

Now some extension can be easily pointed out. From the mechanical point of view, one could consider external excitation. Hence it would be interesting to deal with Eq. (15) modified by an external field of the form $\gamma \cos(\Omega t)$ and to investigate controlability. Another point of view has not been taken into account here: Our numerical procedures are based upon analytical calculation and they are not pure numerical schemes. Thus it is possible to locate "exactly" discontinuity times and to calculate the values of the coordinates at these times. It would be interesting to investigate numerical schemes that can be provided by the mathematical frame and to compare the results with those of the previous sections. Indeed, analytical calculations are not always possible, for instance when smooth polynomial nonlinearities perturb the equations of the Chua system. Then numerical accurate detection of domain transitions would be necessary.

Acknowledgments

The authors would like to thank E. Mussillon for her helpful suggestions.

References

Awrejcewicz, J. & Delfs, J. [1990a] "Dynamics of a self-excited stick-slip oscillator with two degrees of freedom, Part I. Investigation of equilibria," *European J. Mech. A/Solids* **9**(4), 269–282.

Awrejcewicz, J. & Delfs, J. [1990b] "Dynamics of a self-excited stick-slip oscillator with two degrees of freedom. Part II. Slip-stick, slip-slip, stick-slip transitions, periodic and chaotic orbits," *European J. Mech. A/Solids* **9**(5), 397–418.

Brezis, H. [1973] *Opérateurs Maximaux Monotones et semi-groupes de contraction dans les espaces de Hilbert*, Mathematics Studies 5 (North-Holland, Amsterdam).

Capecchi, D. & Vestroni, F. [1995] "Asymptotic response of a two DOF elastoplastic system under harmonic excitation. Internal resonance case," *Nonlin. Dyn.* **7**, 317–333.

Chua, L. O., Komuro, M. & Matsumoto, T. [1986] "The double scroll family. Parts I and II," *IEEE Trans. Circuits Syst.* **CAS-33**, 1072–1118.

Collet, P. & Eckmann, J. [1980] *Iterated Maps on the Interval as Dynamical Systems* (Birkhauser, Basel).

Coullet, P. & Tresser, C. [1984] "Un scénario typique de transition vers le chaos: la cascade de dédoublement de période," *Journal de mécanique théorique et appliquée* Numéro spécial, 217–240 (ISSN 0750-7240).

Crouzeix, M. & Mignot, A. L. [1974], *Analyse Numérique des équations différentielles* (Masson, Paris).

Deimling, K. [1992] *Multivalued differential equations* (W. de Gruyter, Berlin).

Dowell, E. H. & Schwartz, H. B. [1983] "Forced response of a cantilever beam with a dry friction damper attached. Part I: Theory; Part II: Experiment," *J. Sound Vib.* **91**(2), 255–291.

Feigenbaum, M. J. [1978] "Quantitative universality for a class of nonlinear transformations," *J. Stat. Phys.* **19**, 25–52.

Ferri, A. A. & Bindemann, A. C. [1995] "Large amplitude vibration of a beam restrained by a nonlinear sleeve joint," *J. Sound Vib.* **184**(1), 19–34.

Hsu, C. S. [1987] *Cell-to-Cell Mapping* (Springer, NY).

Komuro, M., Tokunaga, R., Matsumoto, T., Chua, L. O. & Hotta, A. [1991] "Global bifurcation analysis of the double scroll circuit," *Int. J. Bifurcation and Chaos* **1**, 139–182.

Kuznetsov, A. P., Kuznetsov, S. P., Sataev, I. R. & Chua, L. O. [1996] "Multi-parameter criticality in Chua's circuit at period doubling transition to chaos," *Int. J. Bifurcation and Chaos* **6**(1), 119–148.

Lamarque, C.-H. & Malasoma, J.-M. [1992] "Computation of basin of attraction for three coexisting attractors," *European J. Mech. A/Solids* **11**(6), 781–790.

Li, T. Y. & Yorke, J. A. [1975] "Period three implies chaos," *Am. Math. Mon.* **82**, 985–992.

Lorentz, E. N. [1963] "Deterministic nonperiodic flow," *J. Atmos. Sci.* **20**, 130–141.

Lozi, R. [1978] "Un attracteur étrange (?) du type attracteur de Hénon," *Journal de Physique*, 9–10.

Madan, R. N. [1993] *Chua's Circuit: A Paradigm for Chaos. World Scientific Series on Nonlinear Science, Series B*, Vol. 1 (World Scientific, Singapore).

Mahla, A. I. & Badan Palhares, A. G. [1993] "Chua's

circuit with a discontinuous nonlinearity," *J. Circuits, Syst. Comput.* **3**(1), 231–237.

Malasoma J.-M., Lamarque, C.-H. & Jézéquel, L. [1994] "Numerical observation of an intermittent transition from an equilibrium point to a chaotic attractor," *Phys. Lett.* **A186**, 126–132.

Monteiro Marques, M. D. P. [1994] "An existence, uniqueness and regularity study of the dynamics of systems with one-dimensional friction," *European J. Mech. A/Solids* **13**(2), 277–306.

Moreau, J. J. [1988] "Unilateral contact and dry friction in finite freedom dynamics," in *Nonsmooth Mechanics and Applications* (C.I.S.M. Courses and Lectures) eds. Moreau, J. J. & Panagiotopoulos, P. (Springer-Verlag, Berlin), pp. 1–81.

Paoli, L. & Schatzman, M. [1993] "Mouvement à nombre fini de degrés de liberté avec contraintes unilatérales: cas avec perte d'énergie," *Modèl. Math. Anal. Numér.* **27**, 673–717.

Paoli, L., Schatzman, M. & Panet, M. [1992] "Vibrations with an obstacle and finite number of degrees of freedom," in *EUROMECH 280, Proc. Int. Symp. Identification of Nonlinear Mechanical Systems from Dynamic Tests* (Balkema, Rotterdam), pp. 159–164.

Paoli, L. [1993] *Analyse numérique de vibrations avec contraintes unilatérales*, PhD thesis, University of St-Etienne, France.

Pfeiffer, F. & Prestl, W. [1994] "Hammering in diesel-engine driveline systems," *Nonlin. Dyn.* **5**, 477–492.

Popp, K. & Stelter, P. [1990] "Stick-slip vibrations and chaos," *Phil. Trans. R. Soc. Lond.* **A332**, 89–105.

Schatzman, M. [1978] "A class of nonlinear differential equations of second order in time," *Nonlin. Anal. Theor. Methods Appl.* **2**(3), 355–373.

Sharkovski [1964] "Coexistence of the cycles of a continuous mapping of the line into itself," *Ukr. Mat. Zh.* **16**(1), 61–71.

Shaw, S. W. [1986] "On the dynamic response of a system with dry friction," *J. Sound Vib.* **108**(2), 305–325.

Shaw, J. & Shaw, S. W. [1989] "The onset of chaos in a two-degree-of-freedom impacting system," *J. Appl. Mech.* **56**, 168–174.

Sparrow, C. [1982] *Bifurcations in the Lorenz Equations*, Lecture Notes in Applied Mathematics (Springer-Verlag, NY).

Szemplinska-Stupnicka, W., Plaut, R. H. & Hsieh, J.-C. [1989] "Period doubling and chaos in unsymmetric structures under parametric excitation," *J. Appl. Mech.* **56**, 947–952.

Ueda, Y. [1979] "Randomly transitional phenomena in systems governed by Duffing's equation," *J. Stat. Phys.* **20**, 181–196.

Whiston, G. S. [1987] "Global dynamics of a vibro-impacting linear oscillator," *J. Sound Vib.* **118**(3), 395–429.

Appendix 1
Analytical Calculation— Discontinuities at −1 and 1

$$u_1 = \begin{pmatrix} -\alpha(m_0 - m_1 + \varepsilon) \\ 0 \\ 0 \end{pmatrix}$$

$$C_1 = \begin{pmatrix} -\alpha m_1 & \alpha & 0 \\ 1 & -1 & 1 \\ 0 & -\beta & 0 \end{pmatrix}$$

$$C_0 = \begin{pmatrix} -\alpha m_0 & \alpha & 0 \\ 1 & -1 & 1 \\ 0 & -\beta & 0 \end{pmatrix}$$

Let us assume that the eigenvalues of C_0 are $\sigma_1 \pm i\omega_1$ (complex conjugate) and γ_1 (real). We can find $\mathcal{L}_1$

$$\mathcal{L}_1 = \begin{pmatrix} \sigma_1 & -\omega_1 & 0 \\ \omega_1 & \sigma_1 & 0 \\ 0 & 0 & \gamma_1 \end{pmatrix}$$

and T_1 that are defined by

$$\mathcal{L}_1 = T_1^{-1} C_1 T_1$$

— The first column of T_1 is the real part of the eigenvector associated with $\sigma_1 + i\omega_1$.
— Its second column is the imaginary part of the same eigenvector.
— Its third column corresponds to the eigenvector associated with γ_1.
— We decide that the first line of T_1 is $[m_0/m_1 \;\; 0 \;\; m_0/m_1]$.

Appendix 2
Analytical Calculation— Discontinuity at 0

$$u_1' = \begin{pmatrix} -\alpha(m_0 - m_1) \\ 0 \\ 0 \end{pmatrix}$$

$$u_0 = \begin{pmatrix} -\alpha\varepsilon \\ 0 \\ 0 \end{pmatrix}$$

$$C_0' = \begin{pmatrix} -\alpha(m_0 - \varepsilon) & \alpha & 0 \\ 1 & -1 & 1 \\ 0 & -\beta & 0 \end{pmatrix}$$

Let us assume that the eigenvalues of C_0' are $\sigma_0 \pm i\omega_0$ (complex conjugate) and γ_0 (real). We can find $\mathcal{L}_0$

$$\mathcal{L}_0 = \begin{pmatrix} \sigma_0 & -\omega_0 & 0 \\ \omega_0 & \sigma_0 & 0 \\ 0 & 0 & \gamma_0 \end{pmatrix}$$

and T_0 that are defined by

$$\mathcal{L}_0 = T_0^{-1} C_0 T_0$$

— The first column of T_0 is the real part of the eigenvector associated with $\sigma_0 + i\omega_0$.
— Its second column is the imaginary part of the same eigenvector.
— Its third column corresponds to the eigenvector associated with γ_0.
— We decide that the first line of T_0 is $[m_0/(m_0 - \varepsilon) \;\; 0 \;\; m_0/(m_0 - \varepsilon)]$.